Atmos. Chem. Phys. Discuss., 12, 9665–9715, 2012
www.atmos-chem-phys-discuss.net/12/9665/2012/
doi:10.5194/acpd-12-9665-2012
© Author(s) 2012. CC Attribution 3.0 License.

Atmospheric Chemistry and Physics Discussions

This discussion paper is/has been under review for the journal Atmospheric Chemistry and Physics (ACP). Please refer to the corresponding final paper in ACP if available.

Tropospheric bromine chemistry: implications for present and pre-industrial ozone and mercury

J. P. Parrella[1], D. J. Jacob[1], Q. Liang[2,3], Y. Zhang[4], L. J. Mickley[1], B. Miller[1], M. J. Evans[5,6], X. Yang[7,8], J. A. Pyle[7,8], N. Theys[9], and M. Van Roozendael[9]

[1]School of Engineering and Applied Sciences, Harvard University, Cambridge, MA, USA
[2]Universities Space Research Association GESTAR, Columbia, MD, USA
[3]NASA Goddard Space Flight Center, Greenbelt, MD, USA
[4]Department of Atmospheric Sciences, University of Washington, Seattle, Washington, USA
[5]Department of Chemistry, University of York, York, UK
[6]National Centre for Atmospheric Sciences (NCAS), York, UK
[7]National Centre for Atmospheric Sciences (NCAS), Cambridge, UK
[8]Centre for Atmospheric Sciences, Department of Chemistry, University of Cambridge, Cambridge, CB2 1EW, UK
[9]Belgian Institute for Space Aeronomy (IASB-BIRA), Brussels, Belgium

CC BY

Received: 5 April 2012 – Accepted: 5 April 2012 – Published: 16 April 2012

Correspondence to: J. P. Parrella (parrella@fas.harvard.edu)

Published by Copernicus Publications on behalf of the European Geosciences Union.

Discussion Paper | Discussion Paper | Discussion Paper | Discussion Paper |

Abstract

We present a new model for the global tropospheric chemistry of inorganic bromine (Br_y) coupled to oxidant-aerosol chemistry in the GEOS-Chem chemical transport model (CTM). Sources of tropospheric Br_y include debromination of sea-salt aerosol, photolysis and oxidation of short-lived bromocarbons, and transport from the stratosphere. Comparison to a GOME-2 satellite climatology of tropospheric BrO columns shows that the model can reproduce the observed increase of BrO with latitude, the northern mid-latitudes maximum in winter, and the Arctic maximum in spring. This successful simulation is contingent on the HOBr + HBr reaction taking place in aqueous aerosols and ice clouds. Bromine chemistry in the model decreases tropospheric ozone concentrations by < 1–$8\,\mathrm{nmol\,mol^{-1}}$ (6.5 % globally), with the largest effects in the northern extratropics in spring. The global mean tropospheric OH concentration decreases by 4 %. Inclusion of bromine chemistry improves the ability of global models (GEOS-Chem and p-TOMCAT) to simulate observed 19th-century ozone and its seasonality. Bromine effects on tropospheric ozone are comparable in the present-day and pre-industrial atmospheres so that estimates of anthropogenic radiative forcing are minimally affected. Br atom concentrations are 40 % higher in the pre-industrial atmosphere due to lower ozone, which would decrease by a factor of 2 the atmospheric lifetime of elemental mercury against oxidation by Br. This suggests that historical anthropogenic mercury emissions may have mostly deposited to northern mid-latitudes, enriching the corresponding surface reservoirs. The persistent rise in background surface ozone at northern mid-latitudes during the past decades could possibly contribute to the observations of elevated mercury in subsurface waters of the North Atlantic.

1 Introduction

Bromine radicals ($BrO_x \equiv Br + BrO$) are well-known catalysts for ozone destruction in the stratosphere (Clerbaux and Cunnold, 2007), and also drive ozone depletion and

ACPD
12, 9665–9715, 2012

mercury oxidation in polar surface air (Simpson et al., 2007; Steffen et al., 2008). In the stratosphere, bromine radicals originate from photolysis and oxidation of halons and shorter-lived bromocarbons (Clerbaux and Cunnold, 2007; Law and Sturges, 2007). In polar surface air, they originate from photochemistry involving sea salt in aerosol or on sea ice (Simpson et al., 2007; Yang et al., 2008). There is growing evidence that bromine radical chemistry could be important in the background troposphere as well, with remote sensing observations typically reporting 0.5–2 $pmol\,mol^{-1}$ BrO (Harder et al., 1998; Frieß et al., 1999; Fitzenberger et al., 2000; Van Roozendael et al., 2002; Richter et al., 2002; Platt and Hönninger, 2003; Hendrick et al., 2007; Theys et al., 2007, 2011) and aircraft observations reporting several $pmol\,mol^{-1}$ BrO in the free troposphere (Neuman et al., 2010; Salawitch et al., 2010). Chemical transport model (CTM) studies show that ~1 $pmol\,mol^{-1}$ BrO in the background troposphere would drive significant decrease of ozone (von Glasow et al., 2004; Lary, 2005; Yang et al., 2005) and could account for most of the global oxidation of elemental mercury (Holmes et al., 2006, 2010).

Bromine radical chemistry in the troposphere is initiated by the production of gas-phase inorganic bromine (Br_y) from photolysis and oxidation of short-lived bromocarbons and from debromination of sea-salt aerosol (Yang et al., 2005; Kerkweg et al., 2008). Br_y cycles between BrO_x and non-radical reservoirs (principally HBr, HOBr, $BrNO_3$, $BrNO_2$, Br_2) and is eventually lost by deposition. Sea salt aerosol debromination represents the largest source of Br_y to the troposphere, with estimates between 1000 and 6000 $Gg\,Br\,a^{-1}$ constrained by the observed Br depletion in sea-salt aerosol relative to seawater composition (Sander et al., 2003). This source is mainly in the marine boundary layer where Br_y has a short lifetime against deposition. Bromocarbons emitted by the marine biosphere including $CHBr_3$, CH_2Br_2, and CH_3Br can release Br_y in the free troposphere where its lifetime against deposition is much longer. Global emission estimates are in the range 370–1400 $Gg\,Br\,a^{-1}$ for $CHBr_3$ and 57–280 $Gg\,Br\,a^{-1}$ for CH_2Br_2 (Quack and Wallace, 2003; Warwick et al., 2006; Law and Sturges, 2007; Liang et al., 2010; Pyle et al., 2011). CH_3Br also has a large

ACPD
12, 9665–9715, 2012

Tropospheric bromine chemistry

J. P. Parrella et al.

anthropogenic source as an agricultural pesticide (Clerbaux and Cunnold, 2007) and its contribution to tropospheric Br_y production has been estimated at 60–80 Gg Br a^{-1} (Yvon-Lewis et al., 2009). Implementation of these sources in the p-TOMCAT CTM together with relatively well-established gas-phase Br_y chemistry yields a background tropospheric BrO concentration ~ 0.5 pmol mol^{-1}, at the low end of observations (Yang et al., 2005).

Here we incorporate a detailed simulation capability for tropospheric bromine coupled to oxidant-aerosol chemistry in the GEOS-Chem CTM (Bey et al., 2001). We evaluate this simulation with a recent space-based climatology of tropospheric BrO by Theys et al. (2011). We discuss the effects on tropospheric ozone and mercury budgets for the present-day and pre-industrial atmospheres. Several studies have pointed out the inability of current CTMs to reproduce the low surface ozone observations from the turn of the 20th century, suggesting that CTM-based estimates of the anthropogenic radiative forcing from tropospheric ozone are too low (Wang and Jacob, 1998; Kiehl et al., 1999; Mickley et al., 2001; Shindell et al., 2003; Lamarque et al., 2005; Horowitz, 2006). As we will show, inclusion of bromine chemistry helps to correct this apparent model deficiency.

2 GEOS-Chem bromine simulation

The GEOS-Chem CTM (www.geos-chem.org) has been used extensively for studies of global oxidant-aerosol chemistry. A recent description of the model radical chemistry is given in Mao et al. (2010), and a recent evaluation of the global tropospheric ozone simulation with sonde and satellite observations is given in Zhang et al. (2010). We developed a tropospheric bromine simulation capability fully coupled to the standard oxidant-aerosol chemistry mechanism in version 8-02-02 of the model. The simulation includes ten bromine species transported in the model: Br_2, Br, BrO, HBr, HOBr, $BrNO_2$, $BrNO_3$, $CHBr_3$, CH_2Br_2, and CH_3Br. Here we describe the relevant emissions, chemistry, and deposition. All GEOS-Chem simulations presented here have

ACPD
12, 9665–9715, 2012

horizontal resolution of 4° latitude × 5° longitude, 47 vertical layers extending from the surface to ∼ 80 km in altitude, and an external chemical time step of 1 h. Transport is driven by GEOS-5 assimilated meteorological fields for 2007 from the NASA Global Modeling and Assimilation Office (GMAO). The chemical mechanism is integrated with the SMVGEAR solver for all tropospheric gridboxes (Jacobson and Turco, 1994; Bey et al., 2001). Linear chemistry with climatological rates is used for the stratosphere (Bey et al., 2001), including improved treatment of ozone chemistry with the Linoz parameterization (McLinden et al., 2000). Stratospheric Br_y concentrations are specified from a model climatology as described below.

2.1 Tropospheric sources of Br_y

Tropospheric Br_y is produced in the model by debromination of sea salt aerosol (SSA), photolysis of $CHBr_3$, and oxidation of $CHBr_3$, CH_2Br_2, and CH_3Br by OH (Table 1). SSA observations indicate typically a 50 % loss of bromide (Br^-) relative to seawater composition, implying release to the atmosphere as Br_y (Sander et al., 2003). This release may take place by various reactions producing Br_2, BrCl, or HOBr (Vogt et al., 1996; Sander et al., 1999, 2003), all of which rapidly photolyze to release BrO_x radicals. We treat SSA debromination following the Yang et al. (2005) observation-based parameterization of Br^- depletion factors relative to seawater for particles in the 1–10 µm diameter range. These depletion factors are applied to the size-dependent SSA source function in GEOS-Chem (Alexander et al., 2005). The resulting Br_y is released as Br_2 uniformly through the depth of the marine boundary layer (MBL) diagnosed from the GEOS-5 meteorological data. Uncertainty in this source will be discussed in Sect. 3. Though SSA debromination is the largest source of tropospheric Br_y in GEOS-Chem, removal by deposition in the MBL is fast. We find that this source contributes 48 % of Br_y in the global free troposphere, the rest originating from bromocarbons.

$CHBr_3$ and CH_2Br_2 are emitted from oceanic macroalgae and phytoplankton (Quack and Wallace, 2003; Yokouchi et al., 2005; Butler et al., 2007), and are thought to be the dominant bromocarbon precursors for tropospheric Br_y (Warwick et al., 2006; Law and

ACPD
12, 9665–9715, 2012

CC BY

Sturges, 2007). We use emission estimates from Liang et al. (2010) for different latitudinal bands and including enhancements in coastal regions (Carpenter et al., 1999), based on ship cruise data (Quack and Wallace, 2003; Warwick et al., 2006) and refined with airborne observations (Liang et al., 2010). The Liang et al. (2010) emission estimates are aseasonal, but we add seasonality to the $CHBr_3$ source in the northern extratropics (> 30° N) as described below to better match observations. Both $CHBr_3$ and CH_2Br_2 in the model are removed by oxidation by OH, and $CHBr_3$ is in addition removed by photolysis (Table 2). We compute mean tropospheric lifetimes for $CHBr_3$ and CH_2Br_2 of 21 days and 91 days respectively (Table 1).

We evaluated our simulations of $CHBr_3$ and CH_2Br_2 with observations from NASA aircraft campaigns previously used by Liang et al. (2010) in the evaluation of their GEOS Climate Chemistry Model (GEOS CCM) simulation. We sampled GEOS-Chem results as averages for the coherent spatial domains of each campaign and for the appropriate months, following the standard methodology used for model evaluation of other species (Bey et al., 2001; Fischer et al., 2012). The observations are for years other than our 2007 simulation year but we regard interannual variability as only a small source of error.

Figure 1 shows composite vertical profiles of $CHBr_3$ and CH_2Br_2 concentrations for the tropics and northern extratropics in April-June. The shapes of the vertical profiles test the model vertical transport modulated by atmospheric lifetime, including in particular the delivery to the free troposphere where the lifetime of Br_y against deposition is long. We see from Fig. 1 that observed vertical gradients are steeper for $CHBr_3$ than for CH_2Br_2, and steeper in the extratropics than in the tropics, reflecting the differences in lifetimes. The model reproduces well these observations.

Figure 2 compares seasonal tropospheric columns of $CHBr_3$ and CH_2Br_2 in the tropics and northern extratropics for the ensemble of NASA aircraft campaigns. This provides a test of emissions in the model. We find that the aseasonal emissions of $CHBr_3$ from Liang et al. (2010) overestimate $CHBr_3$ columns in the northern extratropics during winter and spring, and therefore we apply a seasonal correction factor to these

Discussion Paper | Discussion Paper | Discussion Paper | Discussion Paper |

ACPD

12, 9665–9715, 2012

Tropospheric bromine chemistry

J. P. Parrella et al.

emissions as shown in the figure. No systematic bias is otherwise apparent for $CHBr_3$ in the tropics or for CH_2Br_2. Our global $CHBr_3$ source is 407 Gg Br a^{-1} globally (compared to 425 Gg Br a^{-1} in Liang et al., 2010). Pyle et al. (2011) recently estimated a global $CHBr_3$ source of 380 Gg Br a^{-1} constrained with observations from the OP3 campaign over the maritime continent. Our global CH_2Br_2 source is 57 Gg Br a^{-1}, same as Liang et al. (2010).

CH_3Br has a sufficiently long lifetime to be well-mixed in the troposphere. Surface air observations from the NOAA/GMD global network show a near-uniform concentration of 6–9 pmol mol^{-1} (Montzka et al., 2003) and we use these as lower boundary condition in the model: 6.7 pmol mol^{-1} in the Southern Hemisphere and 8.5 pmol mol^{-1} in the Northern Hemisphere. The implied tropospheric source of Br_y to balance the computed CH_3Br sink in GEOS-Chem is 56 Gg Br a^{-1}, slightly lower than a previous estimate of 63–78 Gg Br a^{-1} (Saltzman et al., 2004).

Halons and other bromocarbons photolyzed or oxidized in the stratosphere represent an additional source of Br_y to the troposphere. This is treated here as an upper boundary condition above the local model tropopause using archived Br_y concentrations from the Liang et al. (2010) stratospheric simulation with the GEOS-5 CCM. The mean stratospheric Br_y concentration in that simulation is 22 pmol mol^{-1}. We use monthly mean 3-D concentration data from Liang et al. (2010) for individual Br_y species, separately for daytime and nighttime. The resulting cross-tropopause source of tropospheric Br_y in GEOS-Chem is 36 Gg Br a^{-1}, as determined by difference with a sensitivity simulation using a zero-concentration upper boundary condition for all Br_y species above the tropopause.

Other tropospheric Br_y sources are neglected as unimportant on a global scale. Kerkweg et al. (2008) estimated that photo-oxidation of bromocarbons other than $CHBr_3$, CH_2Br_2, and CH_3Br accounts for 24 Gg Br a^{-1} of tropospheric Br_y. Pyle and Mather (2009) estimated a global volcanic source of 5–15 Gg Br a^{-1}. Photochemical bromine release from sea ice and salt beds can lead to high local concentrations of BrO in surface air (Stutz et al., 2002; Simpson et al., 2007) but the volumes affected are negligible on a global scale.

2.2 Chemical cycling of Br_y

Table 2 lists the chemical mechanism for tropospheric bromine in GEOS-Chem. Rate constants, heterogeneous reaction coefficients, and photolysis cross-sections are taken from Sander et al. (2010) unless otherwise specified. Photolysis rates are calculated online with the Fast-J radiative transfer model (Wild et al., 2000). Heterogeneous bromine chemistry in aerosols includes hydrolysis of $BrNO_3$ (R29) and reaction between HOBr and HBr (R30). Both are treated with a standard reactive uptake probability (γ) formulation, resulting in an effective gas-phase loss rate constant to a monodisperse aerosol (radius a) given by

$$k = \left(\frac{a}{D} + \frac{4}{v\gamma}\right)^{-1} A. \tag{1}$$

Here D is the molecular diffusion coefficient in air, v is the mean molecular speed of the gas, and A is the aerosol surface area concentration per unit volume of air ($cm^2\,cm^{-3}$) (Schwartz, 1986; Jacob, 2000). GEOS-Chem simulates explicitly the mass concentrations of different aerosol types, and we integrate k over the prescribed relative humidity-dependent size distributions as described by Martin et al. (2002). For $BrNO_3$ hydrolysis (R29) on liquid cloud droplets, the cloud surface area concentration A is calculated from GEOS-5 liquid water content data, assuming effective droplet radii of 10 µm and 6 µm for marine and continental clouds, respectively (Park et al., 2004; Fu et al., 2008). For HBr + HOBr (R30) on ice cloud surfaces, we use $A = 2 \times 10^{-4} I^{0.9}\,cm^2\,cm^{-3}$ (Lawrence and Crutzen, 1998) applied to the local ice water content I ($cm^3\,cm^{-3}$) from the GEOS-5 data.

Reaction (R30) is an important pathway for recycling bromine radicals in the troposphere (von Glasow et al., 2004; Yang et al., 2010). Although the kinetics are uncertain, there is substantial evidence for this reaction. Abbatt (1995) measured $\gamma > 0.25$

ACPD
12, 9665–9715, 2012

Tropospheric bromine chemistry

J. P. Parrella et al.

CC BY

for HBr + HOBr in sulfuric acid solution (69 wt. %) with HBr present in excess. Laboratory measurements show that HOBr reactive uptake on deliquescent NaBr and NaCl aerosol has $\gamma > 0.2$ for pH < 7 (Abbatt and Waschewsky, 1998; Fickert et al., 1999; Wachsmuth et al., 2002). Fickert et al. (1999) determined the relative production of Br_2 vs. BrCl for HOBr reacting with aqueous salt solutions containing both Br^- and Cl^-, and found ≥ 90 % $Br_{2(g)}$ production for $[Br^-]/[Cl^-]$ ratios typical of seawater. Mochida et al. (1998) measured $\gamma = 0.18 \pm 0.02$ for HOBr reactive uptake on solid KBr. On ice surfaces with excess HBr, Abbatt (1994) measured $\gamma = 0.12 \pm 0.03$ for HOBr + HBr at 228 K, and Chaix et al. (2000) measured $\gamma = 0.15 \pm 0.03$ at 205 K. Based on this ensemble of evidence and the recommendation of Sander et al. (2010), we assume that Reaction (R30) proceeds with $\gamma = 0.2$ for sulfate and sea salt aerosol (presumed aqueous) and $\gamma = 0.1$ for ice surfaces, where γ is applied to the locally limiting reactant.

2.3 Sinks of Br_y

Individual Br_y species are removed by wet and dry deposition. Wet deposition in GEOS-Chem takes place by scavenging in convective updrafts and by in- and below-cloud scavenging from large-scale and convective precipitation (Liu et al., 2001). A standard test for wet deposition in global CTMs is simulation of ^{210}Pb aerosol, for which the source and atmospheric concentrations are relatively well constrained (Balkanski et al., 1993). Our version of GEOS-Chem yields a tropospheric lifetime of ^{210}Pb against deposition of 9.5 days (L.T. Murray, personal communication), consistent with a best observational estimate of 9 days (Liu et al., 2001).

Different gas scavenging efficiencies are used in GEOS-Chem for warm liquid clouds ($T > 268$ K), mixed clouds ($248\,K < T < 268$ K), and cold ice clouds ($T < 248$ K). For warm clouds, partitioning into the aqueous phase is determined by the Henry's law constant (Table 2e) and the liquid volume fraction of the precipitating water. Precipitation in mixed clouds is assumed to take place by riming, and the scavenging efficiency depends on the retention efficiency when the cloud droplets freeze (Stuart and Jacobson, 2003). For HBr we assume a 100 % riming retention efficiency, following

ACPD
12, 9665–9715, 2012

CC BY

recommendations from Stuart and Jacobson (2003) for gases with large effective Henry's Law constants. For other Br_y species we assume no retention during riming. We find little sensitivity to the assumed retention efficiency, consistent with previous GEOS-Chem studies for scavenging of ammonia (Wang et al., 2008; Fisher et al., 2010). We assume no scavenging from cold clouds. HBr and HOBr undergo heterogeneous chemistry at the surface of ice particles as discussed in Sect. 2.2.

Dry deposition velocities are calculated locally in GEOS-Chem following a standard resistance-in-series model with surface resistance determined by the Henry's law constant, surface type, and meteorological conditions (Wesely, 1989; Wang et al., 1998). The resulting global annual mean deposition velocities are $0.94\,\mathrm{cm\,s^{-1}}$ for $BrNO_3$, $0.93\,\mathrm{cm\,s^{-1}}$ for HBr, and $0.40\,\mathrm{cm\,s^{-1}}$ for HOBr.

3 Global budget of tropospheric Br_y

Figure 3 shows the global annual mean budget and cycling of tropospheric Br_y in our simulation. The BrO concentration is $0.32\,\mathrm{pmol\,mol^{-1}}$, which implies a daytime mean of $0.64\,\mathrm{pmol\,mol^{-1}}$ since nighttime concentrations are near zero. This is at the low end of the oft-cited (but poorly constrained) 0.5–$2\,\mathrm{pmol\,mol^{-1}}$ range in the observations; more detailed comparison with satellite observations will be presented in Sect. 4. The global mean Br_y concentration is $3.2\,\mathrm{pmol\,mol^{-1}}$, with HBr and HOBr as the principal reservoirs accounting, respectively for 34 % and 28 % of total Br_y. Br_y has a lifetime of 7 days against deposition, with HBr accounting for 55 % of that sink and HOBr for 40 %. Chemical lifetimes are short relative to deposition; that of HBr (the longest-lived reservoir) is only 6 h. Thus the BrO_x radical concentrations are effectively maintained by chemical recycling from non-radical reservoirs.

We see from Fig. 3 that the HBr + HOBr heterogeneous Reaction (R30) plays an important role in the recycling of BrO_x from HBr. A sensitivity simulation without this reaction indicates a factor of 2 decrease in the BrO concentration to $0.15\,\mathrm{pmol\,mol^{-1}}$,

Discussion Paper | Discussion Paper | Discussion Paper | Discussion Paper |

ACPD

12, 9665–9715, 2012

Tropospheric bromine chemistry

J. P. Parrella et al.

with HBr accounting for 70 % of Br_y; the lifetime of Br_y is shorter in that simulation (5 days) because of the high water solubility of HBr (Table 2e). The importance of Reaction (R30) reflects the comparable concentrations of HBr and HOBr (Fig. 3), as rapid HOBr production by the BrO + HO_2 Reaction (R18) compensates for the much longer lifetime of HBr (6 h) than HOBr (20 min).

Figure 4 shows the zonal annual mean BrO, Br, and Br_y concentrations in the model. The highest concentrations of Br_y and BrO are in the marine boundary layer at southern mid-latitudes due to the large source from sea-salt aerosol debromination. In the rest of the troposphere Br_y is relatively uniform (2–4 pmol mol^{-1}), with a minimum in the tropical upper troposphere due to scavenging in convective updrafts. Concentrations increase with altitude in the stratosphere where the boundary conditions from Liang et al. (2010) are applied.

BrO and Br concentrations in Fig. 4 show a general increase with altitude, and BrO shows in addition an increase with latitude. The budget of BrO is largely that of BrO_x since [BrO] $\gg$ [Br]. From Fig. 3 we see that the dominant sink of BrO_x is the BrO + HO_2 Reaction (R18), which is fastest in the tropical lower troposphere where HO_2 concentrations are highest. The dominant source of Br is photolysis of BrO (Fig. 3), which cancels the latitudinal dependence of BrO concentrations and drives the strong increase of Br concentrations with altitude.

4 Comparison to satellite observations of tropospheric BrO

Figure 5 compares simulated BrO tropospheric columns to a GOME-2 satellite data set retrieved by Theys et al. (2011) with monthly resolution for 2007 and for six latitudinal bands. Theys et al. (2011) fitted total slant columns of BrO to the solar backscattered radiation spectra. They then removed the stratospheric contribution by using correlations of stratospheric BrO with ozone and NO_2 from the BASCOE 3D-CTM (Theys et al., 2009) and applying these correlations to the local GOME-2 observations of ozone and stratospheric NO_2 columns. They converted the tropospheric slant columns

ACPD
12, 9665–9715, 2012

CC BY

to vertical columns with an air mass factor assuming a Gaussian-shaped vertical distribution of BrO peaking at 6 km altitude. The grey shading in Fig. 5 indicates the total observational error estimated by Theys et al. (2011), including contributions from the air mass factor, surface albedo, cloud fractions, stratospheric BrO column removal, and cloud top heights.

The GOME-2 data are for ~ 09:30 local time (LT) and we sample GEOS-Chem at 09:00–11:00 LT for comparison. GEOS-Chem data in Fig. 5 include both the actual tropospheric vertical columns (red) and the columns corrected for the Theys et al. (2011) air mass factors using their tabulated scattering weights including for partly cloudy scenes. The correction is uncertain because the tabulation of scattering weights is sparse, but the effect is relatively small except at southern mid-latitudes where the model BrO has a large contribution from the boundary layer. Also shown in Fig. 5 are actual tropospheric vertical columns sampled at 09:00–11:00 LT from the p-TOMCAT CTM bromine simulation of Yang et al. (2010), (blue) and from GEOS-Chem without the HBr + HOBr Reaction (R30) (dashed). p-TOMCAT and GEOS-Chem have completely different heritages. Specific differences in the p-TOMCAT simulation of bromine include the use of a smaller rate constant for HBr + HOBr (γ = 0.02 instead of 0.2, and no reaction on cloud ice particles), and consideration of a blowing snow source in polar regions during spring.

The standard GEOS-Chem simulation underestimates the GOME-2 observations by 30 % on a global mean basis, excluding the poles (40 % including the air mass factor correction), but this is marginally significant considering the observation error. The observations show a positive BrO gradient with increasing latitude that is well reproduced in GEOS-Chem contingent on the (R30) HBr + HOBr reaction. Although Reaction (R30) is a photochemical pathway inasmuch as HOBr and HBr are mainly produced photochemically, it is most effective when radiation is weak since aerosol uptake of HOBr competes with HOBr photolysis. Thus the effect of Reaction (R30) for BrO_x recycling is relatively small in the tropics but very large in the extratropics. It has a strong effect on seasonality in the extratropics, enabling GEOS-Chem to reproduce the observed winter

ACPD
12, 9665–9715, 2012

maximum at northern mid-latitudes, in contrast to p-TOMCAT where Reaction (R30) is less important due to a seasonally constant non-sea salt aerosol loading and lower γ.

A major feature in the BrO observations of (Theys et al., 2011) is the strong Arctic spring maximum. This is reproduced by both GEOS-Chem and p-TOMCAT but for different reasons. In GEOS-Chem it is due mainly to Reaction (R30), with the spring shift (relative to the winter maximum at northern mid-latitudes) due to the need for some insolation to drive HOBr production. In p-TOMCAT it is due to the blowing-snow source (Yang et al., 2008, 2010). The Arctic column amounts in GEOS-Chem are dominated by the free troposphere, while those in p-TOMCAT have a large boundary layer contribution. In-situ observations of BrO during the ARCTAS aircraft campaign over Alaska in April 2008 found significant mixing ratios in the free troposphere, with a mean of $\sim 2\,\mathrm{pmol\,mol^{-1}}$ (Salawitch et al., 2010). In comparison, GEOS-Chem simulates a 09:00–17:00 LT mean of $1.3\,\mathrm{pmol\,mol^{-1}}$ BrO for the Arctic free troposphere in April.

Figure 5 shows little seasonal variation of BrO column in the tropics, either in the observations or the models. The models are too low. Observations at southern mid-latitudes show concentrations comparable to northern mid-latitudes (confirming the dominant natural origin of Br_y) but weaker seasonal dependence as might be expected from lower aerosol concentrations to drive (R30). We conducted several additional sensitivity simulations to examine if uncertainties in gas-phase bromine kinetics as estimated by Sander et al. (2010) could account for the 30 % global model underestimate of BrO relative to the Theys et al. (2011) data. We found the effects to be relatively small. The largest response was from the $Br + CH_2O$ Reaction (R5). Decreasing the pre-exponential factor for that reaction by 30 % and increasing the activation energy by 30 % (error standard deviations from Sander et al., 2010) resulted in a 19 % global increase in simulated BrO.

5 Impact on tropospheric ozone and OH

Tropospheric bromine chemistry drives several catalytic cycles for ozone loss in the troposphere. The three most important are:

Mechanism 1: $BrO + HO_2$

$$Br + O_3 \longrightarrow BrO + O_2 \tag{R5}$$

$$BrO + HO_2 \longrightarrow HOBr + O_2 \tag{R14}$$

$$HOBr + h\nu \longrightarrow Br + OH \tag{R25}$$

$$\text{net:} \quad O_3 + HO_2 \longrightarrow OH + 2O_2$$

with closure for the hydrogen oxide radicals ($HO_x \equiv OH + H + HO_2 +$ organic peroxy and oxy radicals) provided for example by oxidation of CO,

$$CO + OH \xrightarrow{O_2} CO_2 + HO_2\,.$$

Mechanism 2: $BrNO_3 + H_2O$

$$Br + O_3 \longrightarrow BrO + O_2 \tag{R5}$$

$$BrO + NO_2 + M \longrightarrow BrNO_3 + M \tag{R20}$$

$$BrNO_3 \xrightarrow{H_2O,\ \text{aerosol}} HOBr + HNO_3 \tag{R29}$$

$$HOBr + h\nu \longrightarrow Br + OH \tag{R25}$$

$$\text{net:} \quad O_3 + NO_2 + H_2O_{(aq)} \longrightarrow O_2 + HNO_3 + OH\,.$$

ACPD
12, 9665–9715, 2012

Tropospheric bromine chemistry

J. P. Parrella et al.

Mechanism 3: $HOBr + HBr$

$$Br + O_3 \longrightarrow BrO + O_2 \tag{R1}$$

$$BrO + HO_2 \longrightarrow HOBr + O_2 \tag{R2}$$

$$Br + RH \xrightarrow{O_2} HBr + RO_2 \tag{R5–R10}$$

$$HOBr + HBr \xrightarrow{\text{aerosol or ice}} Br_2 + H_2O \tag{R30}$$

$$Br_2 + h\nu \longrightarrow 2Br \tag{R23}$$

$$\text{net}: \quad O_3 + HO_2 + RH \longrightarrow O_2 + H_2O + RO_2 .$$

A common step in all three mechanisms is the formation of HOBr, and we can see from Fig. 3 that both sinks of HOBr (photolysis and reaction with HBr) drive ozone loss. Thus Br-catalyzed ozone loss is limited by the rate of HOBr production. The $BrO + HO_2$ Reaction (R14) accounts for 95 % of global tropospheric HOBr production, while $BrNO_3$ hydrolysis accounts for the rest. Since 92 % of HOBr is photolyzed, Mechanism 1 is responsible for about 90 % of Br-catalyzed ozone loss. However, Mechanism 2 has the important secondary effect of providing a sink for NO_x and thus slowing down ozone production.

Table 3 shows the global impact of bromine chemistry on the tropospheric ozone budget. The budget is calculated following standard procedure as that of the odd oxygen family $O_x \equiv O_3 + NO_2 + 2NO_3 + \text{peroxyacylnitrates} + HNO_4 + 3N_2O_5 + HNO_3 + BrO + BrNO_2 + 2BrNO_3$ (Crutzen and Schmailzl, 1983; Wu et al., 2007) to account for fast cycling of minor species with ozone. The tropospheric production rate of ozone in GEOS-Chem decreases by 4.1 % when bromine chemistry is included, and the ozone lifetime decreases by 2.9 %. We find a 6.5 % decrease in the global tropospheric ozone burden. A previous model study by von Glasow et al. (2004) found a larger (10–15 %) effect of bromine chemistry on the tropospheric ozone budget because they imposed higher bromine concentrations. Yang et al. (2010) found bromine to decrease the ozone burden by 25.5 Tg (8.6 %), close to our result of 24 Tg (6.5 %).

Discussion Paper | Discussion Paper | Discussion Paper | Discussion Paper |

ACPD
12, 9665–9715, 2012
Tropospheric bromine chemistry
J. P. Parrella et al.

We see from Table 3 that bromine chemistry also causes a 4 % decrease in the global concentration of OH, the main tropospheric oxidant. This appears to mainly reflect the decreases in ozone and NO_x, and is partly compensated by the source of OH from Mechanism 2. Applying our global mean fields of OH and temperature with kinetics from Sander et al. (2010), we calculate a methylchloroform tropospheric lifetime against oxidation by OH in GEOS-Chem of 4.79 yr with bromine and 4.65 yr without. Though both are shorter than estimates from observations, 5.5 to 6 yr (Spivakovsky et al., 2000; Prinn et al., 2005), bromine decreases the model bias. Fast conversion of HO_2 to H_2O in aerosols, not included in our GEOS-Chem version, could fully correct the bias (Mao et al., 2010, 2012).

Figure 6 shows the seasonal zonal mean decreases in tropospheric ozone concentrations due to bromine chemistry. Concentrations decrease by $< 1–8\,\text{nmol mol}^{-1}$ depending on region and season. The impact is largest in the northern extratropics in spring, reflecting a combination of elevated BrO (Fig. 5) and ozone. The general increase with latitude in the effect of bromine on ozone is consistent with the previous model studies of von Glasow et al. (2004) and Yang et al. (2010). We find little zonal variability in the effect.

A number of studies have previously evaluated the global ozone simulation in GEOS-Chem with observations from surface sites, sondes, and satellites (Sauvage et al., 2007; Nassar et al., 2009; Zhang et al., 2010). These have shown patterns of over- and underestimates that can vary significantly in successive model versions due to changes in model emissions, chemistry, and transport (Wu et al., 2007). Zhang et al. (2010) presented an extensive global comparison to ozonesonde and satellite measurements using a version of GEOS-Chem similar to ours (v8-02-03). They found that the model was too high in southern mid-latitudes and the northern subtropics but too low in the tropics, with negligible bias in the northern extratropics. Adding bromine chemistry in that simulation would produce mixed results in comparisons to observations. However, the latest version of GEOS-Chem (v9; www.geos-chem.org) includes improved isoprene chemistry that corrects the ozone bias in the tropics but drives a systematic model

Discussion Paper | Discussion Paper | Discussion Paper | Discussion Paper |
ACPD
12, 9665–9715, 2012
Tropospheric bromine chemistry
J. P. Parrella et al.

overestimate of 5–10 $nmol\,mol^{-1}$ in the northern extratropics (Paulot et al., 2009a,b). Including bromine chemistry in that latest version could largely correct the discrepancy in the extratropics and this will need to be investigated in future work.

6 Impact on pre-industrial ozone and radiative forcing

A long-standing problem in global modeling of tropospheric ozone has been the inability of models to reproduce the very low ozone concentrations measured in surface air worldwide at the turn of the 20th century (Wang and Jacob, 1998; Mickley et al., 2001; Shindell et al., 2003; Lamarque et al., 2005; Horowitz, 2006). Calibration of these older measurements is controversial (Marenco et al., 1994) but the Montsouris (Paris) measurements are considered reliable (Volz and Kley, 1988). To examine the potential for bromine chemistry to address this discrepancy we conducted a GEOS-Chem sensitivity simulation for the pre-industrial atmosphere removing all anthropogenic sources (including NO_x from fertilizer use), and reducing methane from 1700 $nmol\,mol^{-1}$ to 700 $nmol\,mol^{-1}$. We decreased biomass burning to 10 % of its present value (Wang and Jacob, 1998), though this has little impact on our results. Bromine sources were held to present-day estimates, except for CH_3Br and the stratospheric boundary condition. We used 5 $pmol\,mol^{-1}$ $CHBr_3$ in surface air worldwide based on ice core records (Saltzman et al., 2004). Concentrations of stratospheric Br_y species were scaled from a total of 22 $pmol\,mol^{-1}$ to 12 $pmol\,mol^{-1}$ Br_y (Liang et al., 2010; Montzka et al., 2011).

Figure 7 compares the 1876–1886 Montsouris observations to simulated pre-industrial ozone from GEOS-Chem and p-TOMCAT (Yang et al., 2010), with and without bromine chemistry. p-TOMCAT applies similar conditions to GEOS-Chem for simulating the pre-industrial atmosphere. The simulations without bromine chemistry overestimate the mean observed ozone by 6.2 and 3.1 $nmol\,mol^{-1}$ in GEOS-Chem and p-TOMCAT, respectively. Both simulations show a seasonal maximum in late winter and early spring, which is a standard extratropical feature in models of natural ozone

Discussion Paper | Discussion Paper | Discussion Paper | Discussion Paper |

ACPD

12, 9665–9715, 2012

(Wang and Jacob, 1998; Monks, 2000; Mickley et al., 2001) but is not seen in the Montsouris observations. Including bromine chemistry decreases annual mean ozone at Montsouris by 2.6 and 1.9 $nmol\,mol^{-1}$ in GEOS-Chem and p-TOMCAT, respectively, effectively correcting the overestimate in p-TOMCAT and reducing it substantially in GEOS-Chem. The decrease is least in summer (0.9–1.4 $nmol\,mol^{-1}$) and greatest in winter-spring (2.3–5.1 $nmol\,mol^{-1}$), which suppresses the winter-spring maximum in both models. Although there are significant differences in simulated ozone between GEOS-Chem and p-TOMCAT, the impact of bromine chemistry on both models is consistent.

Saiz-Lopez et al. (2011) recently suggested that halogen chemistry could reduce the radiative forcing from anthropogenic tropospheric ozone since pre-industrial times by $-0.1\,W\,m^{-2}$ or about 30 %. However, they only considered the impact of this chemistry on the present-day atmosphere. Considering that tropospheric halogens are mainly natural, they would also decrease ozone in the pre-industrial atmosphere. We find in GEOS-Chem that although the sources of bromine are similar in the present and pre-industrial atmospheres, the chemistry differs in two principal ways. First, lower methane in the pre-industrial atmosphere leads to lower CH_2O and hence suppressed production of HBr by Reaction (R5). Second, lower aerosol loadings suppress the HBr + HOBr heterogeneous Reaction (R30). These two effects have competing influences on tropospheric BrO and we find in GEOS-Chem that they largely cancel. Thus the effects of bromine chemistry on ozone are similar in the present-day and pre-industrial atmospheres. We find that the increases in the total tropospheric ozone burden from pre-industrial to present are 119 and 113 Tg in the simulations without and with bromine chemistry, respectively. Considering that the radiative forcing from tropospheric ozone depends roughly linearly on the change in burden (Mickley et al., 1999), we conclude that bromine chemistry decreases ozone radiative forcing by about 5 %.

The impact of bromine chemistry on pre-industrial US surface ozone is of interest because this natural background represents a policy reference point for assessing the risk associated with anthropogenic emissions (US Environmental Protection Agency,

ACPD
12, 9665–9715, 2012

2006). Zhang et al. (2011) recently reported a mean natural ozone background in US surface air of $18 \pm 6\,\mathrm{nmol\,mol^{-1}}$ using a high-resolution version of GEOS-Chem. We find in our simulation that bromine chemistry decreases natural surface ozone over the US from $16\,\mathrm{nmol\,mol^{-1}}$ to $13\,\mathrm{nmol\,mol^{-1}}$ on an annual mean basis, i.e., an effect of $3\,\mathrm{nmol\,mol^{-1}}$.

7 Implications for the atmospheric lifetime of mercury

Mercury in the atmosphere is mostly emitted as gaseous Hg(0), and is removed by oxidation followed by rapid deposition of the water-soluble Hg(II) compounds (Lindberg et al., 2007). The observed atmospheric variability of Hg(0) implies a lifetime against deposition of 0.5–1 yr, with a possibly shorter lifetime against oxidation depending on whether atmospheric Hg(II) can be reduced back to Hg(0) (Slemr et al., 1981, 1985; Bergan et al., 1999; Holmes et al., 2010). Most models of atmospheric mercury have assumed that oxidation of Hg(0) is driven by OH and ozone, but these reactions are now thought to be too slow to be of atmospheric relevance (Calvert and Lindberg, 2005; Hynes et al., 2009). Goodsite et al. (2004) showed that rapid oxidation of Hg(0) to Hg(II) by Br atoms could take place by

$$\mathrm{Hg + Br + M \longrightarrow HgBr + M} \tag{R31}$$

$$\mathrm{HgBr \xrightarrow{M} Hg + Br} \tag{R32}$$

$$\mathrm{HgBr + X \xrightarrow{M} HgBrX}, \tag{R33}$$

where X is a radical, such as OH or Br, that converts unstable Hg(I) to stable Hg(II) in a 3-body reaction. Under tropospheric conditions, Reaction (R31) operates in the low-pressure limit whereas Reaction (R33) operates in the high-pressure limit (Goodsite et al., 2004; Donohoue et al., 2006). Using the kinetic data from Goodsite et al. (2004) and Donohue et al. (2006), together with Br concentration fields from the p-TOMCAT model (Yang et al., 2005) and OH fields from GEOS-Chem, Holmes et al. (2006, 2010)

ACPD
12, 9665–9715, 2012
Tropospheric bromine chemistry
J. P. Parrella et al.

showed that oxidation by Br atoms could represent the dominant global atmospheric sink for Hg(0). Here we revisit this calculation using our computed Br concentrations and draw implications for possible changes in the Hg(0) atmospheric lifetime between pre-industrial and present conditions.

The lifetime τ of Hg(0) against oxidation to Hg(II) by Reactions (R31)–(R33) is given by

$$\tau = \frac{k_{32} + k_{33,\mathrm{Br}}[\mathrm{Br}] + k_{33,\mathrm{OH}}[\mathrm{OH}]}{k_{31}[\mathrm{Br}][\mathrm{M}](k_{33,\mathrm{Br}}[\mathrm{Br}] + k_{33,\mathrm{OH}}[\mathrm{OH}])}, \tag{2}$$

where we have assumed that X in Reaction (R33) can be either Br or OH, following Holmes et al. (2006, 2010). Using the kinetic data of Holmes et al. (2010) and assuming a uniform tropospheric Hg(0) concentration, we derive from our GEOS-Chem model fields a global tropospheric Hg(0) lifetime of 0.33 yr against oxidation. In comparison, Holmes et al. (2010) calculated a lifetime of 0.5 yr in a GEOS-Chem Hg(0) simulation using the Yang et al. (2005) Br concentrations in the free troposphere and assuming 1 pmol mol^{-1} BrO in the marine boundary layer. We repeated our calculation using their archived Br and OH fields and obtain a lifetime of 0.41 yr, which can be viewed as consistent in view of the uncertainty involved with assuming a uniform Hg(0) concentration. Our 20 % shorter lifetime (0.33 vs. 0.41 yr) reflects a 13 % greater mean tropospheric Br concentration in our GEOS-Chem simulation. The response of the lifetime to change in Br concentration is more than linear because thermal decomposition of HgBr (R32) competes with Reaction (R33). We see from Eq. (2) that the response would be quadratic ($\tau \sim 1/[\mathrm{Br}]^2$) in the limit where Reaction (R32) dominates over Reaction (R33) ($k_{32} \gg k_{33}[\mathrm{X}]$) and Reaction (R33) mainly involves reaction with Br ($k_{33,\mathrm{Br}}[\mathrm{Br}] \gg k_{33,\mathrm{OH}}[\mathrm{OH}]$).

The mean tropospheric Br atom concentration in our pre-industrial simulation is 38 % greater than present-day due to lower ozone suppressing the Br + O_3 Reaction (R4). This increase in Br causes the Hg(0) lifetime against oxidation to decrease to 0.19 yr, 42 % lower than present-day. Our work thus suggests that the increase in ozone since

ACPD
12, 9665–9715, 2012

cc BY

pre-industrial times may have increased the atmospheric residence time of Hg(0) by 70 %. With an atmospheric lifetime of only two months, mercury in pre-industrial times would be much less of a global pollutant than today; mercury emitted at northern mid-latitudes would mostly be deposited there. Most of the observed increase in ozone has taken place since 1950 (Marenco et al., 1994), by which time there had already been large anthropogenic mercury emissions at northern mid-latitudes from mining, industry and combustion (Streets et al., 2011).

Slemr et al. (2011) recently reported a 20–38 % worldwide decrease in mercury in surface air over the 1996–2010 period. This cannot be explained by global tropospheric ozone trends, which are inconsistent and weak over that period (Oltmans et al., 2006; Chipperfield et al., 2007; Logan et al., 2012). However, Soerensen et al. (in preparation) argue that the mercury trend is robust only for the North Atlantic and adjacent land areas. The surface ozone background over the North Atlantic has steadily increased over the past decades (Lelieveld et al., 2004; Oltmans et al., 2006; Derwent et al., 2007; Parrish et al., 2009; Dentener et al., 2010), which would imply a corresponding decrease of Br in the MBL and hence of mercury deposition to the ocean. Most of the mercury deposition to the ocean originates from oxidation in the MBL (Selin et al., 2008; Holmes et al., 2009). The decrease in deposition would then affect the re-emission from the ocean as elemental mercury (Soerensen et al., 2010) and could in this manner contribute to the observed atmospheric decrease and to the observed mercury enrichment in North Atlantic subsurface waters relative to the surface.

8 Conclusions

We have developed a simulation of tropospheric bromine coupled to oxidant-aerosol chemistry in the GEOS-Chem global chemical transport model (CTM). Our goal was to better understand the effect of bromine chemistry on tropospheric ozone and mercury, for both the present and pre-industrial atmospheres.

ACPD
12, 9665–9715, 2012

CC BY

We found that standard gas-phase mechanisms for bromine chemistry are unable to reproduce observed levels of tropospheric BrO, including the latitudinal and seasonal variations reported in the new GOME-2 satellite product of Theys et al. (2011). Considerable improvement is achieved by including in GEOS-Chem the HOBr + HBr reaction in aerosols. This brings model BrO into the observed range and reproduces major features of the satellite observations including the increase with latitude and the seasonal maxima in northern mid-latitudes in winter and in the Arctic in spring. Laboratory studies provide ample evidence for the HOBr + HBr reaction but offer limited quantitative information to constrain models. The reactive uptake probability approach used here ($\gamma = 0.2$ for sulfate and sea-salt aerosols, $\gamma = 0.1$ for ice crystals) is probably too simplistic. There is a need to better characterize this reaction over a range of aerosol types and temperatures relevant to the troposphere.

Tropospheric bromine chemistry in GEOS-Chem decreases the present-day global burden of tropospheric ozone by 6.5 %. This is due in part to loss of NO_x by $BrNO_3$ formation and hydrolysis, and in part to catalytic loss of ozone by HOBr formation and photolysis. Ozone mixing ratios decrease by $< 1–8\,\text{nmol}\,\text{mol}^{-1}$ depending on region and season, with the largest effects in the extratropical Northern Hemisphere in spring. The global mean OH concentration decreases by 4 %. These changes in ozone and OH appear to ameliorate previous GEOS-Chem biases in comparisons to observations, although more work is needed to evaluate the simulation of ozone.

We find that bromine chemistry significantly improves the ability of global models to reproduce surface ozone observations from the turn of the 20th century. BrO concentrations in GEOS-Chem are comparable in the present-day and pre-industrial atmospheres, as the effect of decreased methane (suppressing the BrO_x sink from the CH_2O + Br reaction) is compensated by the effect of decreased aerosol (suppressing the BrO_x source from the HBr + HOBr reaction). Comparison of pre-industrial simulations with the GEOS-Chem and p-TOMCAT CTMs to 1876–1886 observations at Montsouris (France) show mean overestimates of $6\,\text{nmol}\,\text{mol}^{-1}$ in GEOS-Chem and $3\,\text{nmol}\,\text{mol}^{-1}$ in p-TOMCAT without bromine chemistry. Including bromine chemistry

ACPD
12, 9665–9715, 2012

CC BY

has similar effects in both models, fully correcting the bias relative to observations in p-TOMCAT and reducing it by half in GEOS-Chem. It suppresses the winter-spring model maximum, better representing the aseasonal behavior of the observations. Bromine chemistry in GEOS-Chem decreases the natural surface ozone background over the US by 3 $\mathrm{nmol\,mol^{-1}}$ on an annual mean basis, a significant increment when assessing the effect of anthropogenic emissions on ozone exposure. Because the effect of bromine chemistry on ozone is similar in the present-day and pre-industrial atmospheres, the global radiative forcing from anthropogenic tropospheric ozone is negligibly affected.

In contrast to the similarity between BrO concentrations in the pre-industrial troposphere and present-day, we find that Br atom concentrations are 40 % higher (global mean) in the pre-industrial troposphere because of lower ozone. It has been hypothesized that Br could provide the main atmospheric oxidant for conversion of elemental mercury Hg(0) to Hg(II), with a linear-to-quadratic dependence on Br concentrations (Holmes et al., 2006, 2010). If so, anthropogenic ozone would have an important impact on the atmospheric lifetime of mercury. Based on best estimates for Hg-Br kinetics, we find in GEOS-Chem that the lifetime of Hg(0) against oxidation to Hg(II) by Br atoms was 2 months in the pre-industrial atmosphere as compared to 4 months at present. Most of the anthropogenic increase in tropospheric ozone has taken place since 1950, and background surface ozone concentrations at northern mid-latitudes have continued to increase in recent decades. Thus historical mercury emissions from human activity (mining, industry, combustion) may not have dispersed globally to the extent previously thought, but instead deposited mostly to the northern mid-latitudes. This could possibly explain observations of elevated mercury in North Atlantic subsurface waters (Soerensen et al., 2010) and the recent trend of decreasing atmospheric concentrations over the North Atlantic. It should be emphasized, however, that the role of Br as a global mercury oxidant remains hypothetical. Our results stress the need for further research to better establish this role.

ACPD
12, 9665–9715, 2012

Acknowledgements. This work was funded by the NASA Atmospheric Composition Modeling and Analysis Program and by the Atmospheric Chemistry Program of the National Science Foundation. J.A.P. and X.Y. thank NERC and NCAS for funding.

References

Abbatt, J. P. D.: Heterogeneous reaction of HOBr with HBr and HCl on ice surfaces at 228 K, Geophys. Res. Lett., 21, 665–668, doi:10.1029/94gl00775, 1994.

Abbatt, J. P. D.: Interactions of HBr, HCl, and HOBr with supercooled sulfuric acid solutions of stratospheric composition, J. Geophys. Res., 100, 14009–14017, doi:10.1029/95jd01367, 1995.

Abbatt, J. P. D. and Waschewsky, G. C. G.: Heterogeneous Interactions of HOBr, HNO_3, O_3, and NO_2 with deliquescent NaCl aerosols at room temperature, J. Phys. Chem. A, 102, 3719–3725, doi:10.1021/jp980932d, 1998.

Alexander, B., Park, R. J., Jacob, D. J., Li, Q. B., Yantosca, R. M., Savarino, J., Lee, C. C. W., and Thiemens, M. H.: Sulfate formation in sea-salt aerosols: constraints from oxygen isotopes, J. Geophys. Res., 110, D10307, doi:10.1029/2004jd005659, 2005.

Arnaud, P.: Cours de chimie organique, 3 edn., Gauthier-Villars, Paris, 1966.

Atkinson, R., Baulch, D. L., Cox, R. A., Hampson, R. F., Rossi, M. J., and Troe, J.: Evaluated kinetic and photochemical data for atmospheric chemistry: supplement VIII, J. Phys. Chem. Ref. Data, 29, 167–266, 2000a.

Atkinson, R., Baulch, D. L., Cox, R. A., Hampson, R. F., Rossi, M. J., and Troe, J.: Evaluated kinetic and photochemical data for atmospheric chemistry. Supplement IX, Heterogeneous chemistry, non-reactive uptake, available at: http://www.iupac-kinetic.ch.cam.ac.uk/, 2000b.

Balkanski, Y. J., Jacob, D. J., Gardner, G. M., Graustein, W. C., and Turekian, K. K.: Transport and residence times of tropospheric aerosols inferred from a global three-dimensional simulation of ^{210}Pb, J. Geophys. Res., 98, 20573–20586, doi:10.1029/93jd02456, 1993.

Beckwith, R. C., Wang, T. X., and Margerum, D. W.: Equilibrium and kinetics of bromine hydrolysis, Inorg. Chem., 35, 995–1000, doi:10.1021/ic950909w, 1996.

Bergan, T., Gallardo, L., and Rodhe, H.: Mercury in the global troposphere: a three-dimensional model study, Atmos. Environ., 33, 1575–1585, 1999.

CC BY

Bey, I., Jacob, D. J., Yantosca, R. M., Logan, J. A., Field, B. D., Fiore, A. M., Li, Q., Liu, H. Y., Mickley, L. J., and Schultz, M. G.: Global modeling of tropospheric chemistry with assimilated meteorology: model description and evaluation, J. Geophys. Res., 106, 23073–23095, 2001.

Butler, J. H., King, D. B., Lobert, J. M., Montzka, S. A., Yvon-Lewis, S. A., Hall, B. D., Warwick, N. J., Mondeel, D. J., Aydin, M., and Elkins, J. W.: Oceanic distributions and emissions of short-lived halocarbons, Global Biogeochem. Cy., 21, GB1023, doi:10.1029/2006gb002732, 2007.

Calvert, J. G. and Lindberg, S. E.: Mechanisms of mercury removal by O_3 and OH in the atmosphere, Atmos. Environ., 39, 3355–3367, 2005.

Carpenter, L. J., Sturges, W. T., Penkett, S. A., Liss, P. S., Alicke, B., Hebestreit, K., and Platt, U.: Short-lived alkyl iodides and bromides at Mace Head, Ireland: links to biogenic sources and halogen oxide production, J. Geophys. Res., 104, 1679–1689, 1999.

Chaix, L., Allanic, A., and Rossi, M. J.: Heterogeneous chemistry of HOBr on different types of ice and on ice doped with HCl, HBr, and HNO_3 at $175\,K < T < 215\,K$, J. Phys. Chem. A, 104, 7268–7277, doi:10.1021/jp001018z, 2000.

Chipperfield, M. P., Fioletov, V. E. (Coordinating Lead Authors), Bregman, B., Burrows, J., Connor, B. J., Haigh, J. D., Harris, N. R. P., Hauchecorne, A., Hood, L. L., Kawa, S. R., Krzyscin, J. W., Logan, J. A., Muthama, N. J., Polvani, L., Randel, W. J., Sasaki, T., Stähelin, J., Stolarski, R. S., Thomason, L. W., and Zawodny, J. M.: Global ozone: past and present, in: Scientific Assessment of Ozone Depletion: 2006, Chapt. 3, Global Ozone Research and Monitoring Project-Report No. 50, World Meteorological Organization, Geneva, Switzerland, 2007.

Clerbaux, C., Cunnold, D. M. (Coordinating Lead Authors), Anderson, J., Engel, A., Fraser, P. J., Mahieu, E., Manning, A., Miller, J., Montzka, S. A., Nassar, R., Prinn, R., Reimann, S., Rinsland, C. P., Simmonds, P., Verdonik, D., Weiss, R., Wuebbles, D., and Yokouchi, Y.: Long-lived compounds, in: Scientific Assessment of Ozone Depletion: 2006, Chapt. 1, Global Ozone Research and Monitoring Project-Report No. 50, World Meteorological Organization, Geneva, Switzerland, 2007.

Crutzen, P. J. and Schmailzl, U.: Chemical budgets of the stratosphere, Planet. Space Sci., 31, 1009–1032, 1983.

Dean, J. A.: Lange's Handbook of Chemistry, McGraw-Hill, Inc., 1992.

ACPD
12, 9665–9715, 2012

Tropospheric bromine chemistry

J. P. Parrella et al.

CC BY

Dentener, F., Keating, T., and Akimoto, H. (Eds.): Ozone and Particulate Matter, Part A, in: Task Force on Hemispheric Transport of Air Pollution 2010, United Nations Economic Commission for Europe, New York, 2010.

Derwent, R. G., Simmonds, P. G., Manning, A. J., and Spain, T. G.: Trends over a 20-yr period from 1987 to 2007 in surface ozone at the atmospheric research station, Mace Head, Ireland, Atmos. Environ., 41, 9091–9098, 2007.

Donohoue, D. L., Bauer, D., Cossairt, B., and Hynes, A. J.: Temperature and pressure dependent rate coefficients for the reaction of Hg with Br and the reaction of Br with Br: a pulsed laser photolysis-pulsed laser induced fluorescence study, J. Phys. Chem. A, 110, 6623–6632, doi:10.1021/jp054688j, 2006.

Fickert, S., Adams, J. W., and Crowley, J. N.: Activation of Br_2 and BrCl via uptake of HOBr onto aqueous salt solutions, J. Geophys. Res., 104, 23719–23727, doi:10.1029/1999jd900359, 1999.

Fischer, E. V., Jacob, D. J., Millet, D. B., Yantosca, R. M., and Mao, J.: The role of the ocean in the global atmospheric budget of acetone, Geophys. Res. Lett., 39, L01807, doi:10.1029/2011gl050086, 2012.

Fisher, J. A., Jacob, D. J., Purdy, M. T., Kopacz, M., Le Sager, P., Carouge, C., Holmes, C. D., Yantosca, R. M., Batchelor, R. L., Strong, K., Diskin, G. S., Fuelberg, H. E., Holloway, J. S., Hyer, E. J., McMillan, W. W., Warner, J., Streets, D. G., Zhang, Q., Wang, Y., and Wu, S.: Source attribution and interannual variability of Arctic pollution in spring constrained by aircraft (ARCTAS, ARCPAC) and satellite (AIRS) observations of carbon monoxide, Atmos. Chem. Phys., 10, 977–996, doi:10.5194/acp-10-977-2010, 2010.

Fitzenberger, R., Bösch, H., Camy-Peyret, C., Chipperfield, M. P., Harder, H., Platt, U., Sinnhuber, B., M, Wagner, T., and Pfeilsticker, K.: First profile measurements of tropospheric BrO, Geophys. Res. Lett., 27, 2921–2924, doi:10.1029/2000gl011531, 2000.

Frenzel, A., Scheer, V., Sikorski, R., George, C., Behnke, W., and Zetzsch, C.: Heterogeneous Interconversion Reactions of $BrNO_2$, $ClNO_2$, Br_2, and Cl_2, J. Phys. Chem. A, 102, 1329–1337, doi:10.1021/jp973044b, 1998.

Frieß, U., Chipperfield, M. P., Harder, H., Otten, C., Platt, U., Pyle, J., Wagner, T., and Pfeilsticker, K.: Intercomparison of measured and modelled BrO slant column amounts for the Arctic winter and spring 1994/95, Geophys. Res. Lett., 26, 1861–1864, doi:10.1029/1999gl900345, 1999.

ACPD
12, 9665–9715, 2012

Tropospheric bromine chemistry

J. P. Parrella et al.

CC BY

Fu, T.-M., Jacob, D. J., Wittrock, F., Burrows, J. P., Vrekoussis, M., and Henze, D. K.: Global budgets of atmospheric glyoxal and methylglyoxal, and implications for formation of secondary organic aerosols, J. Geophys. Res., 113, D15303, doi:10.1029/2007jd009505, 2008.

Goodsite, M. E., Plane, J. M. C., and Skov, H.: A theoretical study of the oxidation of Hg^0 to $HgBr_2$ in the Troposphere, Environ. Sci. Technol., 38, 1772–1776, doi:10.1021/es034680s, 2004.

Haag, W. R. and Hoigne, J.: Ozonation of bromide-containing waters: kinetics of formation of hypobromous acid and bromate, Environ. Sci. Technol., 17, 261–267, doi:10.1021/es00111a004, 1983.

Harder, H., Camy-Peyret, C., Ferlemann, F., Fitzenberger, R., Hawat, T., Osterkamp, H., Schneider, M., Perner, D., Platt, U., Vradelis, P., and Pfeilsticker, K.: Stratospheric BrO profiles measured at different latitudes and seasons: Atmospheric observations, Geophys. Res. Lett., 25, 3843–3846, doi:10.1029/1998gl900026, 1998.

Hendrick, F., Van Roozendael, M., Chipperfield, M. P., Dorf, M., Goutail, F., Yang, X., Fayt, C., Hermans, C., Pfeilsticker, K., Pommereau, J.-P., Pyle, J. A., Theys, N., and De Mazière, M.: Retrieval of stratospheric and tropospheric BrO profiles and columns using ground-based zenith-sky DOAS observations at Harestua, 60° N, Atmos. Chem. Phys., 7, 4869–4885, doi:10.5194/acp-7-4869-2007, 2007.

Holmes, C. D., Jacob, D. J., and Yang, X.: Global lifetime of elemental mercury against oxidation by atomic bromine in the free troposphere, Geophys. Res. Lett., 33, L20808, doi:10.1029/2006gl027176, 2006.

Holmes, C. D., Jacob, D. J., Mason, R. P., and Jaffe, D. A.: Sources and deposition of reactive gaseous mercury in the marine atmosphere, Atmos. Environ., 43, 2278–2285, 2009.

Holmes, C. D., Jacob, D. J., Corbitt, E. S., Mao, J., Yang, X., Talbot, R., and Slemr, F.: Global atmospheric model for mercury including oxidation by bromine atoms, Atmos. Chem. Phys., 10, 12037–12057, doi:10.5194/acp-10-12037-2010, 2010.

Horowitz, L. W.: Past, present, and future concentrations of tropospheric ozone and aerosols: Methodology, ozone evaluation, and sensitivity to aerosol wet removal, J. Geophys. Res., 111, D22211, doi:10.1029/2005JD006937, 2006.

Hynes, A. J., Donohoue, D. L., Goodsite, M. E., Hedgecock, I. M., Pirrone, N., and Mason, R.: Our current understanding of major chemical and physical processes affecting mercury dynamics in the atmosphere and at the air-water/terrestrial interfaces, in: Mercury Fate and

CC BY

Transport in the Global Atmosphere, Chap. 14, edited by: Pirrone, N. and Mason, R. P., Springer, 427–457, 2009.

Jacob, D. J.: Heterogeneous chemistry and tropospheric ozone, Atmos. Environ., 34, 2131–2159, 2000.

Jacobson, M. Z. and Turco, R. P.: SMVGEAR: a sparse-matrix, vectorized gear code for atmospheric models, Atmos. Environ., 28, 273–284, 1994.

Kerkweg, A., Jöckel, P., Warwick, N., Gebhardt, S., Brenninkmeijer, C. A. M., and Lelieveld, J.: Consistent simulation of bromine chemistry from the marine boundary layer to the stratosphere – Part 2: Bromocarbons, Atmos. Chem. Phys., 8, 5919–5939, doi:10.5194/acp-8-5919-2008, 2008.

Kiehl, J. T., Schneider, T. L., Portmann, R. W., and Solomon, S.: Climate forcing due to tropospheric and stratospheric ozone, J. Geophys. Res., 104, 31239–31254, doi:10.1029/1999jd900991, 1999.

King, K. D., Golden, D. M., and Benson, S. W.: Kinetics of the gas-phase thermal bromination of acetone. Heat of formation and stabilization energy of the acetonyl radical, J. Am. Chem. Soc., 92, 5541–5546, doi:10.1021/ja00722a001, 1970.

Lamarque, J.-F., Hess, P., Emmons, L., Buja, L., Washington, W., and Granier, C.: Tropospheric ozone evolution between 1890 and 1990, J. Geophys. Res., 110, D08304, doi:10.1029/2004JD005537, 2005.

Lary, D. J.: Halogens and the chemistry of the free troposphere, Atmos. Chem. Phys., 5, 227–237, doi:10.5194/acp-5-227-2005, 2005.

Law, K. S., Sturges, W. T., (Coordinating Lead Authors), Blake, D. R., Blake, N. J., Burkholder, J. B., Butler, J. H., Cox, R. A., Haynes, P. H., Ko, M. K. W., Kreher, K., Mari, C., Pfeilsticker, K., Plane, J. M. C., Salawitch, R. J., Schiller, C., Sinnhuber, B.-M., von Glasow, R., Warwick, N. J., Wuebbles, D. J., and Yvon-Lewis, S. A.: Halogenated very short-lived substances, in: Scientific Assessment of Ozone Depletion: 2006, Chapt. 2, Global Ozone Research and Monitoring Project-Report No. 50, World Meteorological Organization, Geneva, Switzerland, 2007.

Lawrence, M. G. and Crutzen, P. J.: The impact of cloud particle gravitational settling on soluble trace gas distributions, Tellus B, 50, 263–289, 1998.

Lelieveld, J., van Aardenne, J., Fischer, H., de Reus, M., Williams, J., and Winkler, P.: Increasing ozone over the Atlantic Ocean, Science, 304, 1483–1487, doi:10.1126/science.1096777, 2004.

Liang, Q., Stolarski, R. S., Kawa, S. R., Nielsen, J. E., Douglass, A. R., Rodriguez, J. M., Blake, D. R., Atlas, E. L., and Ott, L. E.: Finding the missing stratospheric Br_y: a global modeling study of $CHBr_3$ and CH_2Br_2, Atmos. Chem. Phys., 10, 2269–2286, doi:10.5194/acp-10-2269-2010, 2010.

Lin, J.-T., McElroy, M. B., and Boersma, K. F.: Constraint of anthropogenic NO_x emissions in China from different sectors: a new methodology using multiple satellite retrievals, Atmos. Chem. Phys., 10, 63–78, doi:10.5194/acp-10-63-2010, 2010.

Lindberg, S., Bullock, R., Ebinghaus, R., Engstrom, D., Feng, X., Fitzgerald, W., Pirrone, N., Prestbo, E., and Seigneur, C.: A synthesis of progress and uncertainties in attributing the sources of mercury in deposition, AMBIO, 36, 19–33, 2007.

Liu, H., Jacob, D. J., Bey, I., and Yantosca, R. M.: Constraints from ^{210}Pb and ^{7}Be on wet deposition and transport in a global three-dimensional chemical tracer model driven by assimilated meteorological fields, J. Geophys. Res., 106, 12109–12128, doi:10.1029/2000jd900839, 2001.

Logan, J. A., Staehelin, J., Megretskaia, I. A., Cammas, J.-P., Thouret, V., Claude, H., De Backer, H., Steinbacher, M., Scheel, H. E., Stubi, R., Frohlich, M., and Derwent, R. G.: Changes in ozone over Europe since 1990: analysis of ozone measurements from sondes regular aircraft (MOZAIC) and alpine surface sites, J. Geophys. Res., doi:10.1029/2011JD016952, in press, 2012.

Mao, J., Jacob, D. J., Evans, M. J., Olson, J. R., Ren, X., Brune, W. H., Clair, J. M. St., Crounse, J. D., Spencer, K. M., Beaver, M. R., Wennberg, P. O., Cubison, M. J., Jimenez, J. L., Fried, A., Weibring, P., Walega, J. G., Hall, S. R., Weinheimer, A. J., Cohen, R. C., Chen, G., Crawford, J. H., McNaughton, C., Clarke, A. D., Jaeglé, L., Fisher, J. A., Yantosca, R. M., Le Sager, P., and Carouge, C.: Chemistry of hydrogen oxide radicals (HO_x) in the Arctic troposphere in spring, Atmos. Chem. Phys., 10, 5823–5838, doi:10.5194/acp-10-5823-2010, 2010.

Mao, J., Fan, S.-M., and Jacob, D. J.: Radical loss in the atmosphere from Cu-Fe redox coupling in aerosol, Nature, in review, 2012.

Marenco, A., Gouget, H., Nédélec, P., Pagés, J.-P., and Karcher, F.: Evidence of a long-term increase in tropospheric ozone from Pic du Midi data series: consequences: positive radiative forcing, J. Geophys. Res., 99, 16617–16632, 1994.

Martin, R. V., Jacob, D. J., Logan, J. A., Bey, I., Yantosca, R. M., Staudt, A. C., Li, Q., Fiore, A. M., Duncan, B. N., Liu, H., Ginoux, P., and Thouret, V.: Interpretation of TOMS observations of

ACPD
12, 9665–9715, 2012

Tropospheric bromine chemistry

J. P. Parrella et al.

tropical tropospheric ozone with a global model and in situ observations, J. Geophys. Res., 107, 4351, doi:10.1029/2001jd001480, 2002.
McGrath, M. P. and Rowland, F. S.: Ideal gas thermodynamic properties of HOBr, J. Phys. Chem., 98, 4773–4775, doi:10.1021/j100069a001, 1994.
McLinden, C. A., Olsen, S. C., Hannegan, B., Wild, O., Prather, M. J., and Sundet, J.: Stratospheric ozone in 3-D models: a simple chemistry and the cross-tropopause flux, J. Geophys. Res., 105, 14653–14665, 2000.
Mickley, L. J., Murti, P. P., Jacob, D. J., Logan, J. A., Koch, D. M., and Rind, D.: Radiative forcing from tropospheric ozone calculated with a unified chemistry-climate model, J. Geophys. Res., 104, 30153–30172, doi:10.1029/1999jd900439, 1999.
Mickley, L. J., Jacob, D. J., and Rind, D.: Uncertainty in preindustrial abundance of tropospheric ozone: Implications for radiative forcing calculations, J. Geophys. Res., 106, 3389–3399, doi:10.1029/2000jd900594, 2001.
Mochida, M., Akimoto, H., van den Bergh, H., and Rossi, M. J.: Heterogeneous kinetics of the uptake of HOBr on solid alkali metal halides at ambient temperature, J. Phys. Chem. A, 102, 4819–4828, doi:10.1021/jp980849q, 1998.
Monks, P. S.: A review of the observations and origins of the spring ozone maximum, Atmos. Environ., 34, 3545–3561, 2000.
Montzka, S. A., Butler, J. H., Hall, B. D., Mondeel, D. J., and Elkins, J. W.: A decline in tropospheric organic bromine, Geophys. Res. Lett., 30, 1826, doi:10.1029/2003GL017745, 2003.
Montzka, S. A., Reimann, S. (Coordinating Lead Authors), Engel, A., Krüger, K., O'Doherty, S., Sturges, W. T., Blake, D. R., Dorf, M., Fraser, P., Froidevaux, L., Jucks, K. W., Kreher, K., Kurylo, M. J., Mellouki, A., Miller, J., Nielsen, O.-J., Orkin, V. L., Prinn, R. G., Rhew, R., Santee, M. L., Stohl, A., and Verdonik, D.: Ozone-Depleting Substances (OESs) and related chemicals, in: Scientific Assessment of Ozone Depletion: 2010, Chapt. 1, Global Ozone Research and Monitoring Project-Report No. 52, World Meteorological Organization, Geneva, Switzerland, 516 pp., 2011.
Nassar, R., Logan, J. A., Megretskaia, I. A., Murray, L. T., Zhang, L., and Jones, D. B. A.: Analysis of tropical tropospheric ozone, carbon monoxide, and water vapor during the 2006 El Niño using TES observations and the GEOS-Chem model, J. Geophys. Res., 114, D17304, doi:10.1029/2009JD011760, 2009.
Neuman, J. A., Nowak, J. B., Huey, L. G., Burkholder, J. B., Dibb, J. E., Holloway, J. S., Liao, J., Peischl, J., Roberts, J. M., Ryerson, T. B., Scheuer, E., Stark, H., Stickel, R. E., Tanner, D. J.,

and Weinheimer, A.: Bromine measurements in ozone depleted air over the Arctic Ocean, Atmos. Chem. Phys., 10, 6503–6514, doi:10.5194/acp-10-6503-2010, 2010.

Oltmans, S. J., Lefohn, A. S., Harris, J. M., Galbally, I., Scheel, H. E., Bodeker, G., Brunke, E., Claude, H., Tarasick, D., Johnson, B. J., Simmonds, P., Shadwick, D., Anlauf, K., Hayden, K., Schmidlin, F., Fujimoto, T., Akagi, K., Meyer, C., Nichol, S., Davies, J., Redondas, A., and Cuevas, E.: Long-term changes in tropospheric ozone, Atmos. Environ., 40, 3156–3173, 2006.

Orlando, J. J. and Tyndall, G. S.: Rate coefficients for the thermal decomposition of $BrONO_2$ and the heat of formation of $BrONO_2$, J. Phys. Chem., 100, 19398–19405, doi:10.1021/jp9620274, 1996.

Park, R. J., Jacob, D. J., Field, B. D., Yantosca, R. M., and Chin, M.: Natural and transboundary pollution influences on sulfate-nitrate-ammonium aerosols in the United States: Implications for policy, J. Geophys. Res., 109, D15204, doi:10.1029/2003jd004473, 2004.

Parrish, D. D., Millet, D. B., and Goldstein, A. H.: Increasing ozone in marine boundary layer inflow at the west coasts of North America and Europe, Atmos. Chem. Phys., 9, 1303–1323, doi:10.5194/acp-9-1303-2009, 2009.

Paulot, F., Crounse, J. D., Kjaergaard, H. G., Kürten, A., St. Clair, J. M., Seinfeld, J. H., and Wennberg, P. O.: Unexpected epoxide formation in the gas-phase photooxidation of isoprene, Science, 325, 730–733, 2009a.

Paulot, F., Crounse, J. D., Kjaergaard, H. G., Kroll, J. H., Seinfeld, J. H., and Wennberg, P. O.: Isoprene photooxidation: new insights into the production of acids and organic nitrates, Atmos. Chem. Phys., 9, 1479–1501, doi:10.5194/acp-9-1479-2009, 2009b.

Platt, U. and Hönninger, G.: The role of halogen species in the troposphere, Chemosphere, 52, 325–338, 2003.

Prinn, R. G., Huang, J., Weiss, R. F., Cunnold, D. M., Fraser, P. J., Simmonds, P. G., McCulloch, A., Harth, C., Reimann, S., Salameh, P., O'Doherty, S., Wang, R. H. J., Porter, L. W., Miller, B. R., and Krummel, P. B.: Evidence for variability of atmospheric hydroxyl radicals over the past quarter century, Geophys. Res. Lett., 32, L07809, doi:10.1029/2004gl022228, 2005.

Pyle, D. M. and Mather, T. A.: Halogens in igneous processes and their fluxes to the atmosphere and oceans from volcanic activity: a review, Chem. Geol., 263, 110–121, 2009.

Pyle, J. A., Ashfold, M. J., Harris, N. R. P., Robinson, A. D., Warwick, N. J., Carver, G. D., Gostlow, B., O'Brien, L. M., Manning, A. J., Phang, S. M., Yong, S. E., Leong, K. P., Ung, E. H.,

ACPD
12, 9665–9715, 2012

CC BY

and Ong, S.: Bromoform in the tropical boundary layer of the Maritime Continent during OP3, Atmos. Chem. Phys., 11, 529–542, doi:10.5194/acp-11-529-2011, 2011.
Quack, B. and Wallace, D. W. R.: Air-sea flux of bromoform: Controls, rates, and implications, Global Biogeochem. Cy., 17, 1023, doi:10.1029/2002GB001890, 2003.
Richter, A., Wittrock, F., Ladstätter-Weißenmayer, A., and Burrows, J. P.: GOME measurements of stratospheric and tropospheric BrO, Adv. Space Res., 29, 1667–1672, 2002.
Saiz-Lopez, A., Lamarque, J.-F., Kinnison, D. E., Tilmes, S., rdóñez, C., Orlando, J. J., Conley, A. J., Plane, J. M. C., Mahajan, A. S., Sousa Santos, G., Atlas, E. L., Blake, D. R., Sander, S. P., Schauffler, S., Thompson, A. M., and Brasseur, G.: Estimating the climate significance of halogen-driven ozone loss in the tropical marine troposphere, Atmos. Chem. Phys. Discuss., 11, 32003–32029, doi:10.5194/acpd-11-32003-2011, 2011.
Salawitch, R. J., Canty, T., Kurosu, T., Chance, K., Liang, Q., da Silva, A., Pawson, S., Nielsen, J. E., Rodriguez, J. M., Bhartia, P. K., Liu, X., Huey, L. G., Liao, J., Stickel, R. E., Tanner, D. J., Dibb, J. E., Simpson, W. R., Donohoue, D., Weinheimer, A., Flocke, F., Knapp, D., Montzka, D., Neuman, J. A., Nowak, J. B., Ryerson, T. B., Oltmans, S., Blake, D. R., Atlas, E. L., Kinnison, D. E., Tilmes, S., Pan, L. L., Hendrick, F., Van Roozendael, M., Kreher, K., Johnston, P. V., Gao, R. S., Johnson, B., Bui, T. P., Chen, G., Pierce, R. B., Crawford, J. H., and Jacob, D. J.: A new interpretation of total column BrO during Arctic spring, Geophys. Res. Lett., 37, L21805, doi:10.1029/2010gl043798, 2010.
Saltzman, E. S., Aydin, M., De Bruyn, W. J., King, D. B., and Yvon-Lewis, S. A.: Methyl bromide in preindustrial air: measurements from an Antarctic ice core, J. Geophys. Res., 109, D05301, doi:10.1029/2003JD004157, 2004.
Sander, R.: Compilation of Henry's Law Constants for Inorganic and Organic Species of Potential Importance in Environmental Chemistry, available at: http://www.henrys-law.org, 1999.
Sander, R., Rudich, Y., von Glasow, R., and Crutzen, P. J.: The role of $BrNO_3$ in marine tropospheric chemistry: a model study, Geophys. Res. Lett., 26, 2857–2860, 1999.
Sander, R., Keene, W. C., Pszenny, A. A. P., Arimoto, R., Ayers, G. P., Baboukas, E., Cainey, J. M., Crutzen, P. J., Duce, R. A., Hönninger, G., Huebert, B. J., Maenhaut, W., Mihalopoulos, N., Turekian, V. C., and Van Dingenen, R.: Inorganic bromine in the marine boundary layer: a critical review, Atmos. Chem. Phys., 3, 1301–1336, doi:10.5194/acp-3-1301-2003, 2003.
Sander, S. P., Friedl, R. R., Abbatt, J. P. D., Barker, J. R., Burkholder, J. B., Golden, D. M., Kolb, C. E., Kurylo, M. J., Moortgat, G. K., Wine, P. H., Huie, R. E., and Orkin, V. L.: Chemical

CC BY

kinetics and photochemical data for use in atmospheric studies, Evaluation Number 17, NASA Jet Propulsion Laboratory, 2010.

Sauvage, B., Martin, R. V., van Donkelaar, A., Liu, X., Chance, K., Jaeglé, L., Palmer, P. I., Wu, S., and Fu, T.-M.: Remote sensed and in situ constraints on processes affecting tropical tropospheric ozone, Atmos. Chem. Phys., 7, 815–838, doi:10.5194/acp-7-815-2007, 2007.

Scheffler, D., Grothe, H., Willner, H., Frenzel, A., and Zetzsch, C.: Properties of Pure Nitryl Bromide. Thermal Behavior, UV/Vis and FTIR Spectra, and Photoisomerization to trans-BrONO in an Argon Matrix, Inorg. Chem., 36, 335–338, doi:10.1021/ic9606946, 1997.

Schwartz, S. E.: Mass-transport considerations pertinent to aqueous-phase reactions of gases in liquid-water clouds, in: Chemistry of Multiphase Atmospheric Systems, edited by: Jaechske, W., Springer, Heidelberg, 415–471, 1986.

Schweitzer, F., Mirabel, P., and George, C.: Uptake of hydrogen halides by water droplets, J. Phys. Chem. A, 104, 72–76, doi:10.1021/jp992621o, 2000.

Seakins, P. W., Pilling, M. J., Niiranen, J. T., Gutman, D., and Krasnoperov, L. N.: Kinetics and thermochemistry of $R + HBr \leftrightarrow RH + Br$ reactions: determinations of the heat of formation of C_2H_5, /-C_3H_7, sec-C_4H_9, and t-C_4H_9 radicals, J. Phys. Chem., 96, 9847–9855, doi:10.1021/j100203a050, 1992.

Selin, N. E., Jacob, D. J., Yantosca, R. M., Strode, S., Jaeglé, L., and Sunderland, E. M.: Global 3-D land-ocean-atmosphere model for mercury: present-day versus preindustrial cycles and anthropogenic enrichment factors for deposition, Global Biogeochem. Cy., 22, GB2011, doi:10.1029/2007gb003040, 2008.

Shindell, D. T., Faluvegi, G., and Bell, N.: Preindustrial-to-present-day radiative forcing by tropospheric ozone from improved simulations with the GISS chemistry-climate GCM, Atmos. Chem. Phys., 3, 1675–1702, doi:10.5194/acp-3-1675-2003, 2003.

Simpson, W. R., von Glasow, R., Riedel, K., Anderson, P., Ariya, P., Bottenheim, J., Burrows, J., Carpenter, L. J., Frieß, U., Goodsite, M. E., Heard, D., Hutterli, M., Jacobi, H.-W., Kaleschke, L., Neff, B., Plane, J., Platt, U., Richter, A., Roscoe, H., Sander, R., Shepson, P., Sodeau, J., Steffen, A., Wagner, T., and Wolff, E.: Halogens and their role in polar boundary-layer ozone depletion, Atmos. Chem. Phys., 7, 4375–4418, doi:10.5194/acp-7-4375-2007, 2007.

Slemr, F., Seiler, W., and Schuster, G.: Latitudinal distribution of mercury over the Atlantic Ocean, J. Geophys. Res., 86, 1159–1166, doi:10.1029/JC086iC02p01159, 1981.

ACPD
12, 9665–9715, 2012

cc BY

Slemr, F., Schuster, G., and Seiler, W.: Distribution, speciation, and budget of atmospheric mercury, J. Atmos. Chem., 3, 407–434, doi:10.1007/bf00053870, 1985.

Slemr, F., Brunke, E.-G., Ebinghaus, R., and Kuss, J.: Worldwide trend of atmospheric mercury since 1995, Atmos. Chem. Phys., 11, 4779–4787, doi:10.5194/acp-11-4779-2011, 2011.

Soerensen, A. L., Sunderland, E. M., Holmes, C. D., Jacob, D. J., Yantosca, R. M., Skov, H., Christensen, J. H., Strode, S. A., and Mason, R. P.: An improved global model for air-sea exchange of mercury: high concentrations over the North Atlantic, Environ. Sci. Technol., 44, 8574–8580, doi:10.1021/es102032g, 2010.

Soerensen, A. L., Jacob, D. J., Streets, D. G., Witt, M., Ebinghaus, R., Mason, R. P., Andersson, M., and Sunderland, E. M.: Hg^0 trends in the North and South Atlantic Marine Boundary Layer: the importance of the subsurface ocean mercury reservoir, Geophys. Res. Lett., in preparation, 2012.

Spivakovsky, C. M., Logan, J. A., Montzka, S. A., Balkanski, Y. J., Foreman-Fowler, M., Jones, D. B. A., Horowitz, L. W., Fusco, A. C., Brenninkmeijer, C. A. M., Prather, M. J., Wofsy, S. C., and McElroy, M. B.: Three-dimensional climatological distribution of tropospheric OH: Update and evaluation, J. Geophys. Res., 105, 8931–8980, doi:10.1029/1999jd901006, 2000.

Steffen, A., Douglas, T., Amyot, M., Ariya, P., Aspmo, K., Berg, T., Bottenheim, J., Brooks, S., Cobbett, F., Dastoor, A., Dommergue, A., Ebinghaus, R., Ferrari, C., Gardfeldt, K., Goodsite, M. E., Lean, D., Poulain, A. J., Scherz, C., Skov, H., Sommar, J., and Temme, C.: A synthesis of atmospheric mercury depletion event chemistry in the atmosphere and snow, Atmos. Chem. Phys., 8, 1445–1482, doi:10.5194/acp-8-1445-2008, 2008.

Streets, D. G., Devane, M. K., Lu, Z., Bond, T. C., Sunderland, E. M., and Jacob, D. J.: All-time releases of mercury to the atmosphere from human activities, Environ. Sci. Technol., 45, 10485–10491, doi:10.1021/es202765m, 2011.

Stuart, A. L. and Jacobson, M. Z.: A timescale investigation of volatile chemical retention during hydrometeor freezing: Nonrime freezing and dry growth riming without spreading, J. Geophys. Res., 108, 4178, doi:10.1029/2001jd001408, 2003.

Stutz, J., Ackermann, R., Fast, J. D., and Barrie, L.: Atmospheric reactive chlorine and bromine at the Great Salt Lake, Utah, Geophys. Res. Lett., 29, 1380, doi:10.1029/2002gl014812, 2002.

Theys, N., Van Roozendael, M., Hendrick, F., Fayt, C., Hermans, C., Baray, J.-L., Goutail, F., Pommereau, J.-P., and De Mazière, M.: Retrieval of stratospheric and tropospheric BrO

ACPD
12, 9665–9715, 2012

Tropospheric bromine chemistry

J. P. Parrella et al.

CC BY

columns from multi-axis DOAS measurements at Reunion Island (21° S, 56° E), Atmos. Chem. Phys., 7, 4733–4749, doi:10.5194/acp-7-4733-2007, 2007.

Theys, N., Van Roozendael, M., Errera, Q., Hendrick, F., Daerden, F., Chabrillat, S., Dorf, M., Pfeilsticker, K., Rozanov, A., Lotz, W., Burrows, J. P., Lambert, J.-C., Goutail, F., Roscoe, H. K., and De Mazière, M.: A global stratospheric bromine monoxide climatology based on the BASCOE chemical transport model, Atmos. Chem. Phys., 9, 831–848, doi:10.5194/acp-9-831-2009, 2009.

Theys, N., Van Roozendael, M., Hendrick, F., Yang, X., De Smedt, I., Richter, A., Begoin, M., Errera, Q., Johnston, P. V., Kreher, K., and De Mazière, M.: Global observations of tropospheric BrO columns using GOME-2 satellite data, Atmos. Chem. Phys., 11, 1791–1811, doi:10.5194/acp-11-1791-2011, 2011.

US Environmental Protection Agency: Air Quality Criteria for Ozone and Related Photochemical Oxidants (Final), Vols. I, II, and III, 600/R-605/004aF-cF, 2006.

Van Roozendael, M., Wagner, T., Richter, A., Pundt, I., Arlander, D. W., Burrows, J. P., Chipperfield, M., Fayt, C., Johnston, P. V., Lambert, J. C., Kreher, K., Pfeilsticker, K., Platt, U., Pommereau, J. P., Sinnhuber, B. M., Tørnkvist, K. K., and Wittrock, F.: Intercomparison of BrO measurements from ERS-2 GOME, ground-based and balloon platforms, Adv. Space Res., 29, 1661–1666, 2002.

Vogt, R., Crutzen, P. J., and Sander, R.: A mechanism for halogen release from sea-salt aerosol in the remote marine boundary layer, Nature, 383, 327–330, 1996.

Volz, A. and Kley, D.: Evaluation of the Montsouris series of ozone measurements made in the nineteenth century, Nature, 332, 240–242, 1988.

von Glasow, R., von Kuhlmann, R., Lawrence, M. G., Platt, U., and Crutzen, P. J.: Impact of reactive bromine chemistry in the troposphere, Atmos. Chem. Phys., 4, 2481–2497, doi:10.5194/acp-4-2481-2004, 2004.

Wachsmuth, M., Gäggeler, H. W., von Glasow, R., and Ammann, M.: Accommodation coefficient of HOBr on deliquescent sodium bromide aerosol particles, Atmos. Chem. Phys., 2, 121–131, doi:10.5194/acp-2-121-2002, 2002.

Wang, J., Hoffmann, A. A., Park, R. J., Jacob, D. J., and Martin, S. T.: Global distribution of solid and aqueous sulfate aerosols: Effect of the hysteresis of particle phase transitions, J. Geophys. Res., 113, D11206, doi:10.1029/2007jd009367, 2008.

Wang, Y. and Jacob, D.: Anthropogenic forcing on tropospheric ozone and OH since preindustrial times, J. Geophys. Res., 103, 31123–31135, 1998.

ACPD

12, 9665–9715, 2012

Tropospheric bromine chemistry

J. P. Parrella et al.

Wang, Y., Jacob, D. J., and Logan, J. A.: Global simulation of tropospheric O_3-NO_x-hydrocarbon chemistry 1. Model formulation, J. Geophys. Res., 103, 10713–10725, doi:10.1029/98jd00158, 1998.

Warwick, N. J., Pyle, J. A., Carver, G. D., Yang, X., Savage, N. H., O'Connor, F. M., and Cox, R. A.: Global modeling of biogenic bromocarbons, J. Geophys. Res., 111, D24305, doi:10.1029/2006JD007264, 2006.

Wesely, M. L.: Parameterization of surface resistance to gaseous dry deposition in regional-scale numerical models, Atmos. Environ., 23, 1293–1304, 1989.

Wild, O., Zhu, X., and Prather, M. J.: Fast-J: accurate simulation of in- and below-cloud photolysis in tropospheric chemical models, J. Atmos. Chem., 37, 245–282, doi:10.1023/a:1006415919030, 2000.

Wu, S., Mickley, L. J., Jacob, D. J., Logan, J. A., Yantosca, R. M., and Rind, D.: Why are there large differences between models in global budgets of tropospheric ozone?, J. Geophys. Res., 112, D05302, doi:10.1029/2006jd007801, 2007.

Yang, X., Cox, R. A., Warwick, N. J., Pyle, J. A., Carver, G. D., O'Connor, F. M., and Savage, N. H.: Tropospheric bromine chemistry and its impacts on ozone: a model study, J. Geophys. Res., 110, D23311, doi:10.1029/2005JD006244, 2005.

Yang, X., Pyle, J. A., and Cox, R. A.: Sea salt aerosol production and bromine release: role of snow on sea ice, Geophys. Res. Lett., 35, L16815, doi:10.1029/2008GL034536, 2008.

Yang, X., Pyle, J. A., Cox, R. A., Theys, N., and Van Roozendael, M.: Snow-sourced bromine and its implications for polar tropospheric ozone, Atmos. Chem. Phys., 10, 7763–7773, doi:10.5194/acp-10-7763-2010, 2010.

Yokouchi, Y., Hasebe, F., Fujiwara, M., Takashima, H., Shiotani, M., Nishi, N., Kanaya, Y., Hashimoto, S., Fraser, P., Toom-Sauntry, D., Mukai, H., and Nojiri, Y.: Correlations and emission ratios among bromoform, dibromochloromethane, and dibromomethane in the atmosphere, J. Geophys. Res., 110, D23309, doi:10.1029/2005JD006303, 2005.

Yvon-Lewis, S. A., Saltzman, E. S., and Montzka, S. A.: Recent trends in atmospheric methyl bromide: analysis of post-Montreal Protocol variability, Atmos. Chem. Phys., 9, 5963–5974, doi:10.5194/acp-9-5963-2009, 2009.

Zhang, L., Jacob, D. J., Liu, X., Logan, J. A., Chance, K., Eldering, A., and Bojkov, B. R.: Intercomparison methods for satellite measurements of atmospheric composition: application to tropospheric ozone from TES and OMI, Atmos. Chem. Phys., 10, 4725–4739, doi:10.5194/acp-10-4725-2010, 2010.

CC BY

Table 1. Global sources of tropospheric bromine in GEOS-Chem.

Source	Emission, $\mathrm{Gg\,Br\,a^{-1}}$	Lifetime, d*
Sea salt debromination	1420	~ 0
$CHBr_3$	407	21
CH_2Br_2	57	91
CH_3Br	56	402
Transport from stratosphere	36	~ 0

* Global mean tropospheric lifetimes of bromocarbons determining the release of Br_y. Values of ~ 0 are entered for the sea salt debromination and stratospheric sources because these sources are as Br_y.

ACPD
12, 9665–9715, 2012

cc BY

Table 2a. Tropospheric bromine chemistry in GEOS-Chem: bimolecular reactions*.

Reaction number	Reaction	A, cm^3 molecule^{-1} s^{-1}	$-E_a/R$, K
R1	$CHBr_3 + OH \rightarrow 3Br + products$	1.35×10^{-12}	−600
R2	$CH_2Br_2 + OH \rightarrow 2Br + products$	2.00×10^{-12}	−840
R3	$CH_3Br + OH \rightarrow Br + products$	2.35×10^{-12}	−1300
R4	$Br + O_3 \rightarrow BrO + O_2$	1.60×10^{-11}	−780
R5	$Br + CH_2O \xrightarrow{O_2} HBr + HO_2 + CO$	1.70×10^{-11}	−800
R6	$Br + HO_2 \rightarrow HBr + O_2$	4.80×10^{-12}	−310
R7	$Br + CH_3CHO \xrightarrow{O_2} HBr + CH_3CO_3$	1.30×10^{-11}	−360
R8	$Br + (CH_3)_2CO \xrightarrow{O_2} HBr + CH_3C(O)CH_2OO$	1.66×10^{-10}	−7000
R9	$Br + C_2H_6 \xrightarrow{O_2} HBr + C_2H_5OO$	2.36×10^{-10}	−6411
R10	$Br + C_3H_8 \xrightarrow{O_2} HBr + C_3H_7OO$	8.77×10^{-10}	−4330
R11	$Br + BrNO_3 \rightarrow Br_2 + NO_3$	4.90×10^{-11}	0
R12	$Br + NO_3 \rightarrow BrO + NO_2$	1.60×10^{-11}	0
R13	$HBr + OH \rightarrow Br + H_2O$	5.50×10^{-12}	200
R14	$BrO + NO \rightarrow Br + NO_2$	8.80×10^{-12}	260
R15	$BrO + OH \rightarrow Br + HO_2$	1.70×10^{-11}	250
R16	$BrO + BrO \rightarrow 2Br + O_2$	2.40×10^{-12}	40
R17	$BrO + BrO \rightarrow Br_2 + O_2$	2.80×10^{-14}	860
R18	$BrO + HO_2 \rightarrow HOBr + O_2$	4.50×10^{-12}	460
R19	$Br_2 + OH \rightarrow HOBr + Br$	2.10×10^{-11}	240

* The Arrhenius expression for rate constants is $k = A\exp(-E_a/RT)$. Kinetic data are from Sander et al. (2010) except for Reaction (R7) (Atkinson et al., 2000), Reaction (R8) (King et al., 1970), Reactions (R9) and (R10) (Seakins et al., 1992), and Reaction (R11) (Orlando and Tyndall, 1996).

ACPD
12, 9665–9715, 2012

CC BY

Table 2b. Tropospheric bromine chemistry in GEOS-Chem: three-body reactions[a].

Reaction number	Reaction	Rate coefficients[b]
R20	$Br + NO_2 + M \rightarrow BrNO_2 + M$	$k_0 = 4.2 \times 10^{-31}(T/300)^{-2.4}$; $k_\infty = 2.7 \times 10^{-11}$, $F_c = 0.6$
R21	$BrO + NO_2 + M \rightarrow BrNO_3 + M$	$k_0 = 5.2 \times 10^{-31}(T/300)^{-3.2}$; $k_\infty = 6.9 \times 10^{-12}$, $F_c = 0.6$

[a] The rate constant is calculated as $k = \{[k_0[M]/(1 + k_0[M]/k_\infty)] \times F_c^n\}$, where $n = \{1 + (\log_{10}(k_0[M]/k_\infty))^2\}^{-1}$ and [M] is the air number density (molecules cm^{-3}).
[b] From Sander et al. (2010); k_0 and k_∞ have units of cm^6 $molecule^{-2}$ s^{-1} and cm^3 $molecule^{-1}$ s^{-1}, respectively, and T has unit of K.

ACPD
12, 9665–9715, 2012

Table 2c. Tropospheric bromine chemistry in GEOS-Chem: photolysis[a].

Reaction number	Reaction	J, s^{-1} [b]
R22	$CHBr_3 + h\nu \rightarrow 3Br + \text{products}$	1.1×10^{-6}
R23	$Br_2 + h\nu \rightarrow 2Br$	4.2×10^{-2}
R24	$BrO + h\nu \xrightarrow{O_2} Br + O_3$	4.0×10^{-2}
R25	$HOBr + h\nu \rightarrow Br + OH$	2.3×10^{-3}
R26	$BrNO_2 + h\nu \rightarrow Br + NO_2$	1.2×10^{-3}
R27	$BrNO_3 + h\nu \rightarrow BrO + NO_2$	2.2×10^{-4}
R28	$BrNO_3 + h\nu \rightarrow Br + NO_3$	1.2×10^{-3}

[a] Photolysis rates are calculated locally with the Fast-J radiative transfer model (Wild et al., 2000) using absorption cross-sections from Sander et al. (2010) except for Reaction (R26) (Scheffler et al., 1997). All quantum yields are assumed to be 100 % (Sander et al., 2010).
[b] Global annual tropospheric mean photolysis frequencies calculated in GEOS-Chem.

ACPD
12, 9665–9715, 2012

Tropospheric bromine chemistry

J. P. Parrella et al.

Table 2d. Tropospheric bromine chemistry in GEOS-Chem: heterogeneous processes.

Reaction number	Reaction	Reactive uptake probability (γ)[a]
R29	$BrNO_3 \xrightarrow{H_2O(\text{aerosol, cloud})} HOBr + HNO_3$	0.3 (sea salt, liquid cloud)[b], 0.8 (sulfate)[c]
R30	$HOBr + HBr \xrightarrow{\text{aqueous aerosol, ice}} Br_2 + H_2O$	0.2 (sea salt, sulfate), 0.1 (ice)[c]

[a] See Eq. (1) in text.
[b] IUPAC evaluation (Atkinson et al., 2000b).
[c] Sander et al. (2010); for Reaction (R30) the reactive uptake probability is applied to the limiting reactant.

ACPD
12, 9665–9715, 2012

CC BY

Table 2e. Tropospheric bromine chemistry in GEOS-Chem: Henry's law constants[a].

Species	K_H(298), M atm^{-1}	$-\Delta H/R$, K	Reference
HBr	0.75 (7.5×10^{13})[b]	10 200	Schweitzer et al. (2000)
HOBr	6100[c]	6010[d]	Frenzel et al. (1998)
Br_2[e]	0.76	4180	Dean (1992)
Br	1.2	1800	Sander (1999)
BrO[d]	0.71		Frenzel et al. (1998)
$BrNO_2$	0.3		Frenzel et al. (1998)
$BrNO_3$[g]	∞		Sander (1999)

[a] The Henry's law constant is calculated as $K_H(T) = K_H(298) \exp\left[\frac{-\Delta H}{R}\left(\frac{1}{T} - \frac{1}{298}\right)\right]$, where K_H(298) is the value at 298 K, ΔH is the enthalpy of solution, R is the gas constant, and T is the temperature (K).

[b] The Henry's Law constant is from Schweitzer et al. (2000); The value in parentheses is the effective Henry's law constant K_H^* at pH 5 accounting for $HBr_{(aq)}/Br^-$ acid dissociation: $K_H^*(T) = K_H(T)\left(1 + \frac{K_a}{[H^+]}\right)$, where $K_a = 1 \times 10^9$ M is the acid dissociation constant (Arnaud, 1966).

[c] $HOBr_{(aq)}/BrO^-$ acid dissociation is negligible under atmospheric conditions ($K_a = 1.6 \times 10^{-9}$ M; Haag and Hoigne, 1983).

[d] McGrath and Rowland (1994).

[e] Br_2(aq) dissociation by hydrolysis can be neglected (Beckwith et al., 1996).

[f] Estimated by analogy with ClO (Sander et al., 2010).

[g] $BrNO_3$ uptake by liquid clouds is modeled by a reactive uptake probability (Table 2d) and is not limited by Henry's law solubility. For modeling dry deposition an infinite Henry's law constant is assumed.

ACPD
12, 9665–9715, 2012

cc BY

Table 3. Global tropospheric ozone (O_x) budget in GEOS-Chem[a].

	Chemical production, $P(O_x)$ $Tg\,a^{-1}$	Chemical loss, $L(O_x)$ $Tg\,a^{-1}$	Deposition $Tg\,a^{-1}$	STE[b] $Tg\,a^{-1}$	Tropospheric burden Tg	Lifetime days	[OH] 10^6 molecules cm^{-3}
No bromine	5110	4480	948	349	370	27.8	1.23
With bromine	4910	4350	879	355	346	27.0	1.18

[a] Global annual mean budget for the odd oxygen (O_x) chemical family defined as $O_x \equiv O_3 + NO_2 + 2NO_3$ + peroxyacylnitrates + $HNO_4 + 3N_2O_5 + HNO_3 + BrO + BrNO_2 + 2BrNO_3$ (Crutzen and Schmailzl, 1983; Wu et al., 2007), with molecular weight taken to be that of ozone.
[b] Stratosphere-to-troposphere exchange is inferred from mass-balance: STE = $L(O_x)$ + deposition$-P(O_x)$.

Discussion Paper | Discussion Paper | Discussion Paper | Discussion Paper |
ACPD
12, 9665–9715, 2012
Tropospheric bromine chemistry
J. P. Parrella et al.

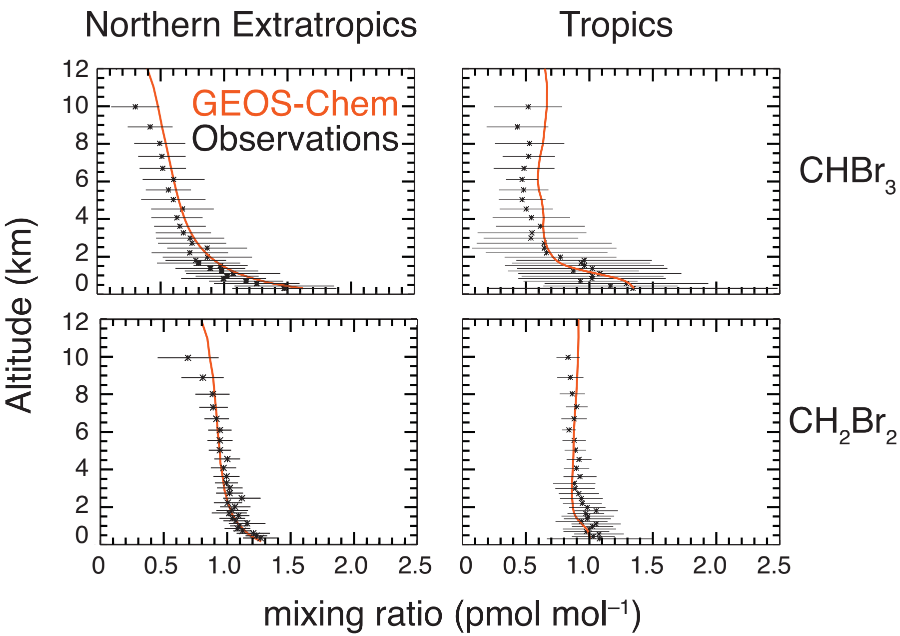

Fig. 1. Mean vertical profiles of $CHBr_3$ and CH_2Br_2 concentrations in the northern extratropics (latitudes > 30° N) and tropics (30° S–30° N) for April–June. GEOS-Chem model results (in red) are compared to observations from NASA aircraft campaigns (in black) including TRACE-P, INTEX-B, and ARCTAS. See Liang et al. (2010) for references on the aircraft observations. Vertical profiles have been averaged over coherent regions for individual missions and then averaged again over the latitudinal domain. Horizontal bars are standard deviations in the original data.

ACPD
12, 9665–9715, 2012

Tropospheric bromine chemistry

J. P. Parrella et al.

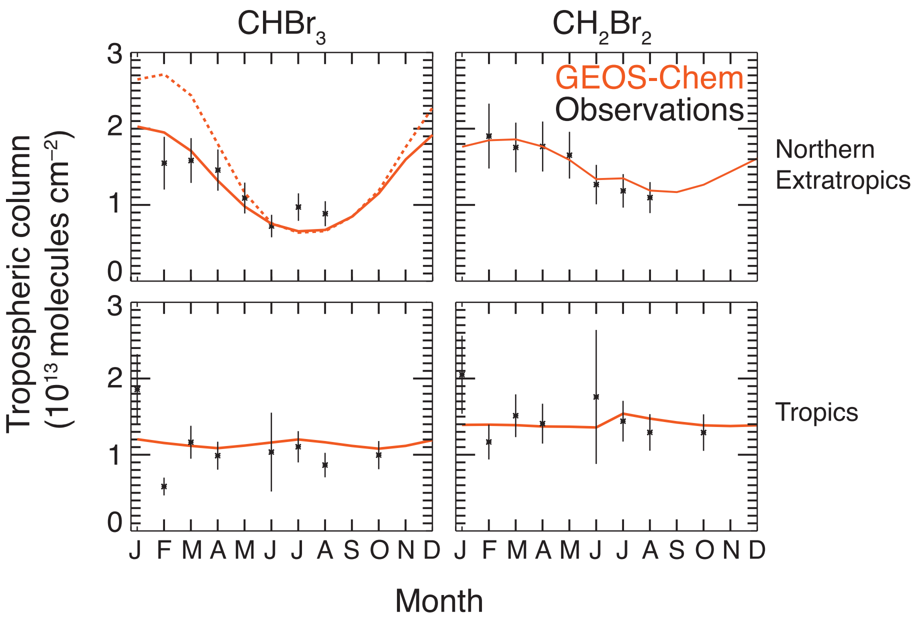

Fig. 2. Comparison of simulated (red) and observed (black) tropospheric columns (molecules cm^{-2}) of CH_2Br_2 and $CHBr_3$, for the northern extratropics (> 30° N) and the tropics (30° S–30° N). Column data are integrals of mean vertical profiles up to 10 km altitude from a compilation of NASA campaigns including STRAT, TRACE-P, INTEX, AVE, TC4, and ARCTAS in the northern extra-tropics and STRAT, PEM-Tropics, TRACE-P, INTEX, Pre-AVE, AVE, and TC4 in the tropics. References for the observations are in Liang et al. (2010). Vertical bars are the standard deviations in the original data. The dashed red line shows the model results for $CHBr_3$ in the northern extratropics using the original aseasonal emissions from Liang et al. (2010); in order to match the observations in GEOS-Chem we applied seasonal scaling factors to $CHBr_3$ emissions in that region (solid red line).

ACPD
12, 9665–9715, 2012

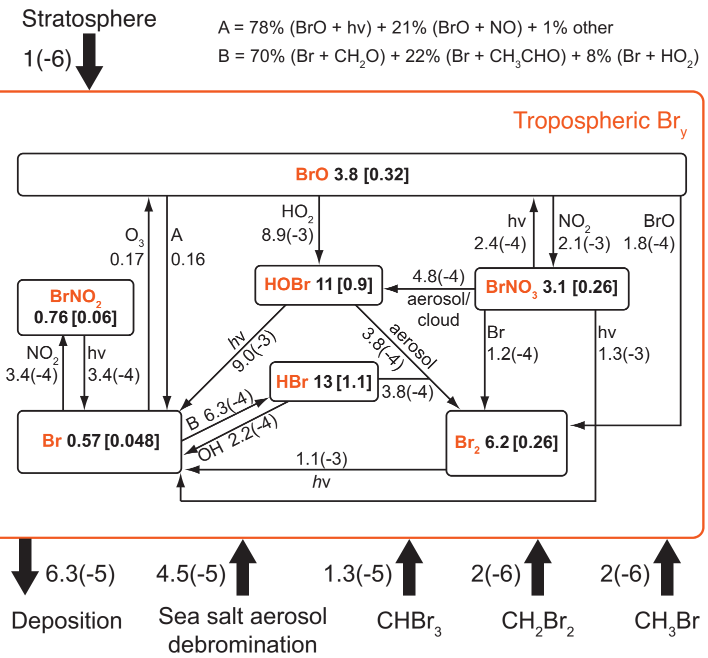

Fig. 3. Global annual mean budget of tropospheric inorganic bromine (Br_y) in GEOS-Chem. The main reactions are indicated. Inventories are given as masses (Gg Br), with mixing ratios (pmol mol^{-1}) in brackets. Rates are given in units of Gg Br s^{-1}. Read 6.3(−5) as 6.3×10^{-5}. All species are in steady state; HBr accounts for 55 % of Br_y loss by deposition, which closes the HBr budget. Sea-salt aerosol debromination is the dominant global source of Br_y but is mainly confined to the marine boundary layer where Br_y has a short lifetime against deposition. It accounts for 48 % of the Br_y source in the global free troposphere.

ACPD
12, 9665–9715, 2012

Tropospheric bromine chemistry

J. P. Parrella et al.

CC BY

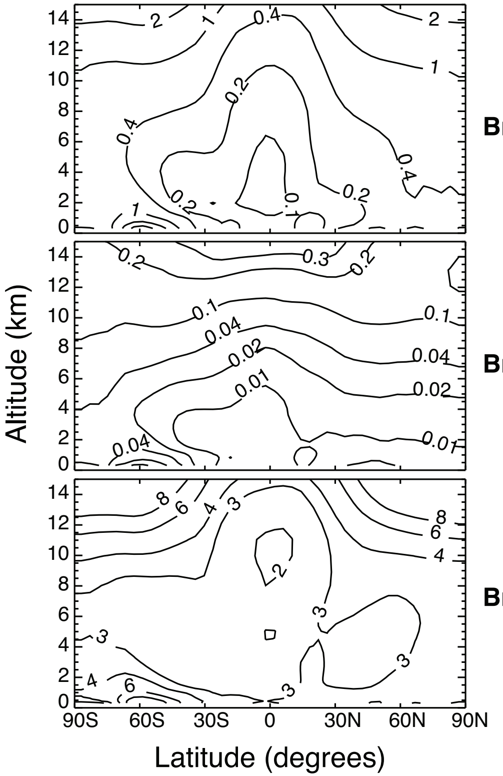

Fig. 4. Zonal annual mean concentrations (pmol mol^{-1}) of BrO, Br, and Br_y in GEOS-Chem.

ACPD
12, 9665–9715, 2012

Tropospheric bromine chemistry

J. P. Parrella et al.

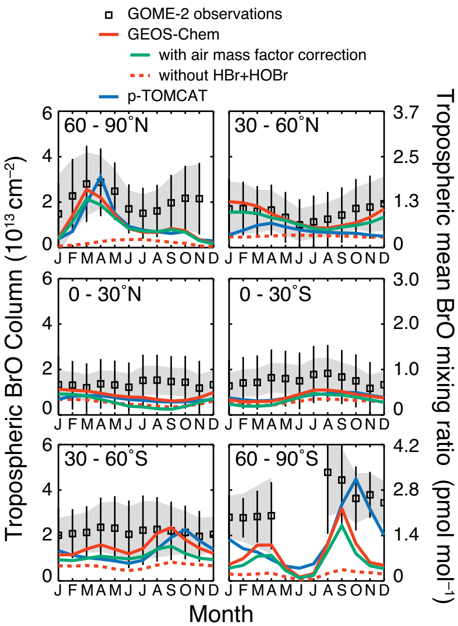

Fig. 5. Seasonal variation of mean tropospheric BrO columns in different latitudinal bands. GOME-2 observations from Theys et al. (2011) are compared to model values from GEOS-Chem and from p-TOMCAT (Yang et al., 2010). GEOS-Chem values are shown for the actual vertical columns (red) and for vertical columns corrected by the GOME-2 air mass factors (green). Also shown are results from a sensitivity simulation without the HBr + HOBr heterogeneous Reaction (R30). p-TOMCAT values are actual vertical columns. The models were sampled at 09:00–11:00 local time (LT), corresponding to the GOME-2 viewing time of ~ 09:30 LT. Grey shading shows the observational error on the means reported by Theys et al. (2011) and vertical bars indicate one standard deviation of their spatial averaging. The BrO mixing ratios on the right axis scale are derived from the BrO columns by dividing by the annual mean tropospheric air density columns for the corresponding latitude bin in GEOS-Chem.

ACPD
12, 9665–9715, 2012

CC BY

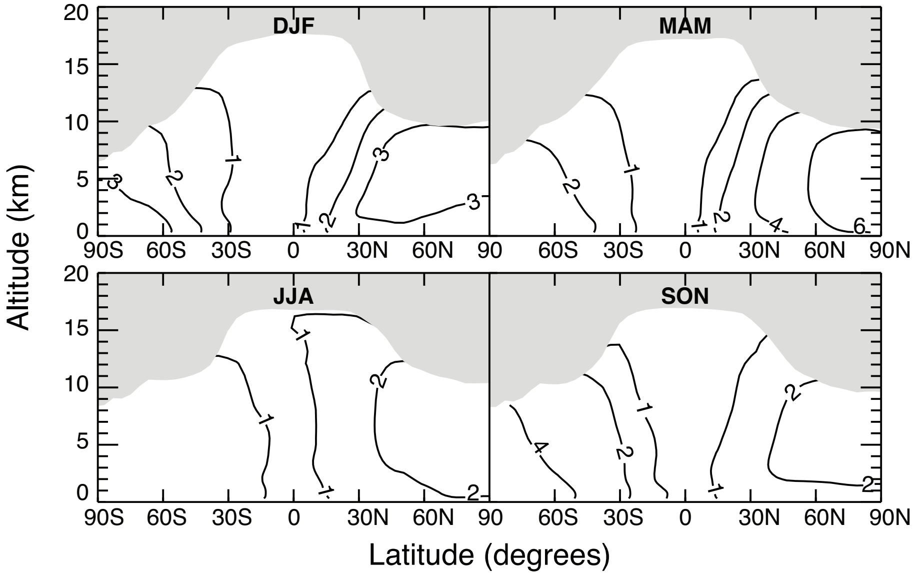

Fig. 6. Decrease in tropospheric ozone ($nmol\,mol^{-1}$) from bromine chemistry. The figure shows zonal seasonal mean differences between GEOS-Chem simulations including vs. not including bromine chemistry. Shading indicates the stratosphere.

ACPD
12, 9665–9715, 2012

Tropospheric bromine chemistry

J. P. Parrella et al.

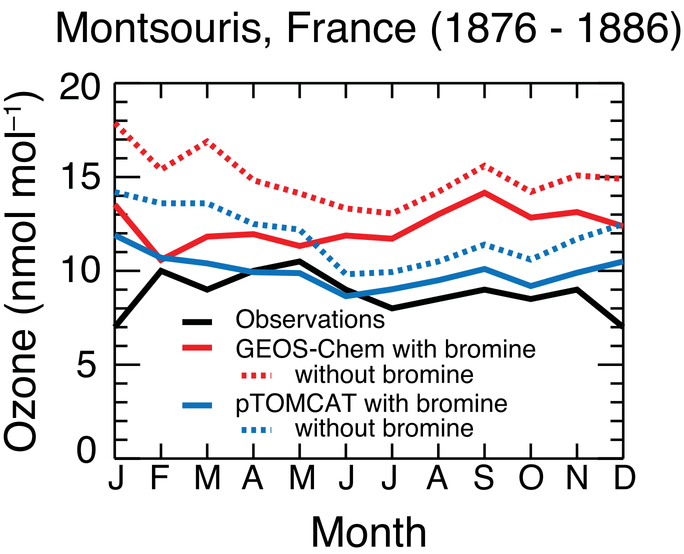

Fig. 7. Mean seasonal variation of 19th-century ozone in surface air at Montsouris, France (50° N, 2° E). 1876–1886 observations re-analyzed by Volz and Kley (1988) (black) are compared to preindustrial model simulations using GEOS-Chem (red) and p-TOMCAT (blue), with bromine chemistry (solid) and without (dotted).

ACPD
12, 9665–9715, 2012